Separation and Purification Technology 349 (2024) 127798

Contents lists available at ScienceDirect

Separation and Purification Technology

journal homepage: www.elsevier.com/locate/seppur

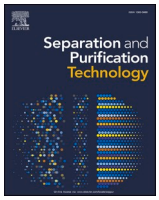

Purification of stilbenes from grape stems in a continuous process based on photo-molecularly imprinted adsorbents and hydroalcoholic solvents

Amir Bzainia [a,d], Getúlio Igrejas [b,c], Maria João V. Pereira [b,c], Mário Rui P.F.N. Costa [d], Rolando C.S. Dias [a,c,*]

[a] Centro de Investigação de Montanha (CIMO), Instituto Politécnico de Bragança, Campus de Santa Apolónia, 5300-253 Bragança, Portugal
[b] Centro de Investigação em Digitalização e Robótica Inteligente (CeDRI), Instituto Politécnico de Bragança, Campus de Santa Apolónia, 5300-253 Bragança, Portugal
[c] Laboratório Associado para a Sustentabilidade e Tecnologia em Regiões de Montanha (SusTEC), Instituto Politécnico de Bragança, Campus de Santa Apolónia, 5300-253 Bragança, Portugal
[d] LSRE, Faculdade de Engenharia, Departamento de Engenharia Química, Universidade do Porto, 4200-465 Porto, Portugal

ARTICLE INFO

Editor: Raquel Aires Barros

Keywords:
Stilbenes
Continuous process
Photo molecularly imprinted polymers
Hydroalcoholic-based purification
Phytochemicals

ABSTRACT

This study presents a sustainable method to purify stilbenes from residual grape stem biomass. This approach was experimentally validated through the use of a pilot size fixed-bed adsorption prototype for the automation of the purification process. Molecularly imprinted polymers, synthesized through photopolymerization at room temperature and incorporating the 4-vinylpyridine monomer, serve as adsorbents. The purification procedure leads to a significant enrichment, with a more than 22-fold increase in (E)-ε-viniferin and a 9-fold increase in (E)-resveratrol. High recoveries of 80.3% and 62.1% for (E)-ε-viniferin and (E)-resveratrol, respectively, were achieved. Notably, the use of eco-friendly water and ethanol mixtures distinguishes this method from others focused on stilbenes purification. This study further explores the variability of the stilbenes in the residual grape stems by analysing different varieties, emphasizing the complexity of the starting material of the purification process. The range of purities achieved for the fractions enriched with stilbenes (e.g., 12.8% for (E)-ε-viniferin and 3.4% for (E)-resveratrol) are suitable for direct use in controlling of *Plasmopara viticola*, the agent causing grapevine downy mildew. Furthermore, through compositional combination of these fractions, it is possible to conceive new stilbene-containing phytochemicals with improved anti-fungal activity. Therefore, the developed adsorbents and purification process, enabling the steady enrichment of stilbenes regardless of the unavoidable variability in the initial vine biomass, is a contribution towards the quest for more environmentally friendly and sustainable phytochemicals.

1. Introduction

Stilbenes, a class of phenolic compounds, have garnered significant attention due to their diverse phytochemical characteristics. The inherent chemical structure of stilbenes endows them with antioxidant, anti-inflammatory and anti-microbial properties which can be harnessed in different fields of applications [1]. In fact, studies have demonstrated the anti-carcinogenic [2,3], antidiabetic [4], and cardioprotective [5] activities of stilbenes. As such, stilbenes are used as food additives (more than 400 products containing resveratrol can be found on the market) [6], for disease treatments [1], or even as ingredients for cosmetic products [7]. The above list of applications is not restrictive and further real-life uses of stilbenes can be consulted in the literature and further references therein [8]. The biosynthesis of stilbenes in plants is reported to be a response to viral, fungal, and bacterial attacks (see e.g., ref [8] for a comprehensive overview of the biosynthesis pathway). Notably, stilbene-enriched extracts, primarily composed of (E)-piceatannol, (E)-resveratrol and (E)-ε-viniferin, have been proven to exhibit antifungal activity [9]. These findings further establish a correlation between the concentration of stilbenes and a decrease in its half maximal inhibitory concentration (IC_{50}). In addition, the stilbenes isolated from grapevine extracts have demonstrated insecticidal efficacy against pest larvae [10]. As a result, stilbenes can play the role of a biological pesticide, thus reducing the use of traditional toxic ones. Such outcomes are

* Corresponding author at: Centro de Investigação de Montanha (CIMO), Instituto Politécnico de Bragança, Campus de Santa Apolónia, 5300-253 Bragança, Portugal.
E-mail address: rdias@ipb.pt (R.C.S. Dias).

https://doi.org/10.1016/j.seppur.2024.127798
Received 12 March 2024; Received in revised form 18 April 2024; Accepted 2 May 2024
Available online 3 May 2024

motivations for the current study, aiming to obtain highly enriched fractions of stilbenes.

These bioactive compounds are found in the different parts of the grapevine, and particularly in the stems part of the grapes (the part where the grape grows) [11,12]. Usually being perceived as byproducts in winemaking, grape stems constitute an abundant and cost-effective biological source of stilbenes [12].

In this context, we propose a new adsorption–desorption process for the refinement of stilbenes from the extracts of grape stems. The process relies on photo-molecularly imprinted adsorbents to produce enriched hydroalcoholic fractions of these compounds. The current work builds upon the preceding findings of our research group, and it is in fact a step closer towards the practical implementation of such technology for the valorization of winemaking residues. In the initial phase, adsorbents were synthesized through photopolymerization and leveraging the molecular imprinting technique (MIT). The synthesized adsorbents, notably incorporating the 4-vinylpyridine (4VP) monomer, were systematically obtained through an experimental design [13]. Several studies have demonstrated the advantage of room temperature photopolymerization over its thermal-based counterpart, emphasizing its ability to preserve the interactions between functional monomers and the template. This preservation directly contributes to the selectivity observed in the final molecularly imprinted polymer [14,15]. The efficiency of the 4VP functional monomer to interact and retain bioactive compounds from vegetal biomass has been demonstrated in several previous studies. Examples of its effectiveness include the purification of flavonoids [16], (E)-resveratrol [17], flavonols and anthocyanins [18]. In addition, the 4VP has shown efficiency in enriching phenolic acids and secoiridoids [19].

In a subsequent publication, the materials' proof of concept was demonstrated via an adsorption–desorption process dedicated to purifying (E)-resveratrol from grape stem extracts. This study showed the aptitude of molecularly imprinted adsorbents to purify the stilbene molecule of (E)-resveratrol from the intricate extract of grape stems [20]. However, a limitation of this study was the utilization of acetonitrile in the purification process, which is classified as a hazardous solvent. Therefore, the currently proposed procedure exclusively involves water and ethanol mixtures to purify the compound of (E)-resveratrol and its derivatives.

Furthermore, as this current study is centered on the valorization of grape stems, it was considered worthwhile to conduct a survey of the stilbenes' content in grape stem varieties originating from the northern regions of Portugal. (E)-resveratrol was selected as a reliable proxy to elucidate the variations in total stilbenes. As a result, this study presents a comprehensive overview of the feedstock utilized in the purification process undertaken herein.

2. Experimental

2.1. Reagents

All chemicals were used as purchased, without further purification. The standard of (E)-resveratrol (≥98 %) was purchased from Cayman (USA). The monomer 4-vinylpyridine (4VP, ≥95 %) was purchased from Alfa Aesar (USA). The styrene monomer (STY, ≥99 %) and the crosslinker ethylene glycol dimethacrylate (EGDMA, ≥98 %) were acquired from Sigma Aldrich (Germany). The polymerization initiator 2,2′- azobis (2-methylpropionitrile) (AIBN, ≥98 %) was purchased from Sigma Aldrich (Germany). The solvent dimethylformamide (DMF, ≥99 %) was purchased from Acros Organics (Belgium). Ethanol (EtOH, ≥99.8 %), methanol (MeOH, ≥99.8 %), acetonitrile (ACN, ≥99.9 %), and glacial acetic acid (AcOH, ≥99.7 %) were all acquired from Fisher Chemical (UK). The water used in the experiments was ultrapure water supplied by the local laboratory.

2.2. Synthesis of photo-molecularly imprinted adsorbents

The synthesis of the photo-molecularly imprinted polymers (MIPs) mirrored methods detailed in our previous study [13], and mainly the photo-polymerizations of the MIP7 and MIP9 were scaled up. Briefly, the polymerization was conducted at room temperature and under UV irradiation. This latter was carried out in a custom-made reactor by Paralab (Portugal). The dispositive is equipped with four mercury vapour lamps (Philips Actinic BL TL 8 W/10 1FM/10X25CC) with a maximum emission at 350 nm. The interior of the reactor is covered with aluminium to reflect the UV light thus making it evenly distributed inside the reactor. The polymerization mixture consisted of 4VP, styrene, EGDMA as monomers, AIBN as initiator and (E)-resveratrol as the imprinting molecule. The optimized recipes of the polymerizations were utilized and are displayed in Table 1. The respective non-imprinted materials were previously synthesized and played the role of the control materials to demonstrate the imprinting of the MIPs. Their upscaled synthesis was not conducted as we have proved in our previous works that the MIPs have higher binding capacities and selectivity towards the target compound [13].

2.3. Material's characterisation

The characterization of the materials was carried out by scanning electron microscopy (SEM) which allowed the examination of their surface morphology. The analysis was conducted at the International Iberian Nanotechnology Laboratory (INL), Braga (Portugal) using the FIB/SEM system HELIOS Nanolab 450S. SEM images were obtained using an electron beam of 3 keV, a beam current of 25 pA and at field free lens mode. Furthermore, Fourier-transform infrared spectroscopy (FTIR) was carried out to provide insights into the chemical composition of the MIPs. In addition, static sorption tests using the standard of (E)-resveratrol were conducted to evaluate the materials' adsorptive properties. Comprehensive details regarding the FTIR and the static sorption tests can be referenced in earlier publications for a more in-depth understanding of the materials' characteristics. [13,20].

2.4. Evaluation of (E)-resveratrol content in grape stems from vineyards in the northern region of Portugal

2.4.1. Grape stems samples

The vineyards that have provided us with grape stems samples are geographically distributed across the northern region of Portugal as shown in Fig. 1. The regions involved in this survey are Minho (M), Douro (D) and Trás-os-Montes (T). Comprehensive details related to the grape stems' samples are summarized in Table 2.

2.4.2. Grape stems extraction procedure

The as received grapes stems were humid, and thus drying was a

Table 1
Photo-polymerization recipes of the molecularly imprinted adsorbents.

Adsorbent	Y_M (%)	Y_{CL} (%)	$Y_{4VP/Res}$	$Y_{STY/Res}$	Y_I (%)	Yield (%)	Solvent
M7	20	60	3/1	1/1	5.2	67.33	ACN-DMF (85:15)
M9	20	40	7/1	1/1	5.2	50.17	ACN-DMF (85:15)

Y_M: Mass fraction of the polymerizable monomers' mixture (including functional monomers and crosslinker) in the polymerization solution;
Y_{CL}: Mole fraction of the crosslinker in the polymerizable monomer's mixture;
$Y_{4VP/Res}$: Mole ratio between 4VP monomer and (E)-resveratrol;
$Y_{STY/Res}$: Mole ratio between (E)-resveratrol and styrene monomer;
Y_I: Mole ratio between the initiator and the polymerizable monomers.

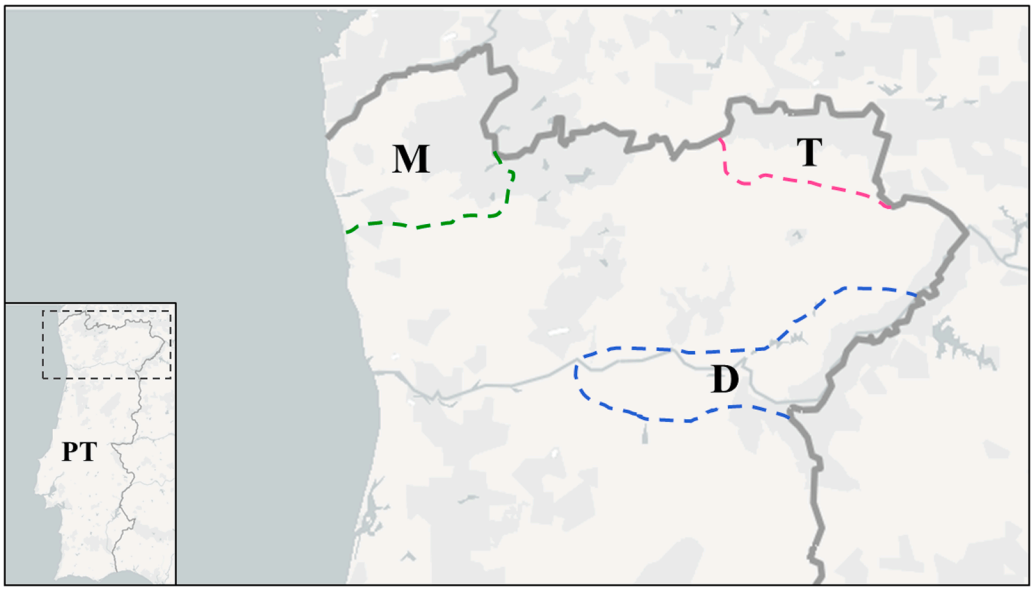

Fig. 1. Vineyard locations of the collected grape stems samples: "M" represents the region of Minho, "T" corresponds to the region of Trás-os-Montes, and "D" denotes the Douro region.

Table 2
Grape stems varieties, origins, and harvest years.

Grape stems	M-1	M-2	D-1	D-2	D-3	T-1	T-2	T-3
Provenance	Minho	Minho	Douro	Douro	Douro	Trás-os-Montes	Trás-os-Montes	Trás-os-Montes
Harvest year	2021	2023	2023	2023	2023	2023	2023	2023

necessary step. For this end, a moderate temperature of 40 °C was used to dry the grape stems (without cutting them into pieces) until no change of mass was noticeable. The dried samples were stored in a dark room with an average temperature of 20 °C. The grape stems were then milled to obtain a homogenous powder. Subsequently, the extraction was carried out using ethanol/water (80:20, v/v) at a ratio of 5 mL of solvent per gram of ground grape stems. The extraction consisted of a 5-minute sonication in an ultrasound bath followed by filtration.

2.4.3. *Extracts' analysis*

The obtained extracts were analysed by high-performance liquid chromatography (HPLC) and the amount of (E)-resveratrol in each grape stems extract was quantified using a calibration curve for the same compound at a wavelength of 280 nm. (E)-ε-viniferin is a dimer of (E)-resveratrol, and thus the same calibration curve was used for its quantification. Details regarding the HPLC as well as the calibration curve (Figure S1) can be consulted in the supplementary material.

2.5. *Fixed-bed adsorption–desorption setup*

The adsorption–desorption experiments were all carried out in an industrial prototype that permits the control and monitoring of the experimental conditions. This prototype features two separate columns that can operate independently. The piping and instrumentation diagram (P&ID) of this prototype is presented in Fig. 2. The prototype is endowed with a dosing pump (Knauer – AZURA P4.1S) and a gradient HPLC pump (Knauer – AZURA P6.1L). The latter permits to perform the desorption using different solvent compositions. A total of four pneumatic 4-way valves (VICI – A90) control the flow path. These valves possess four openings allowing the connection of two inlets to two different outlets and the ability to switch between them if needed (only 3-ways are marked in the scheme). Two of these valves are positioned prior to the columns, while the other two are placed after. The temperature of each column is regulated by a cooling-heating circulator bath (Jubalo 200 F). At the outlet of each column, a UV–vis detector (Sarspec – Flex) is placed to monitor the effluents' absorbances. The prototype is also equipped with a fraction collector (LAMBDA OMNI-COLL) facilitating the recuperation of the desorbed fractions. Furthermore, the different parts of the metallic tubing are surrounded by self-regulating heating cables that allow to raise the temperature of the circuit if needed. In the present work, both columns were used, thus allowing to effectively test two photo-molecularly imprinted adsorbents at once. These materials were packed into stainless-steel chromatography columns of 50 mm × 20 mm, which corresponds to a bed volume of approximately 15.71 mL.

2.6. *Fixed bed adsorption simulation*

The current study focuses on treating crude extracts of grape stems using a fixed-bed adsorption system. To model this process, seven fixed-bed adsorption models were applied to predict the breakthrough curve corresponding to the feeding of the extract into the MIP-packed columns. Their respective mathematical equations are listed in Table 3. Among these models, three use the so-called logistic equation and have been unified as a single model referred to as the "Logistic model" [21]. This logistic model encompasses the Bohart-Adams, the Thomas and the Yoon-Nelson models, the equations of which being summarized in Table 4. The non-linear fitting of the experimental data was performed using the MATLAB® software. Experimental data were collected with a standard fixed-bed adsorption setup (open-loop) and alternatively using recycling (outlet of the column flows into the feed). In each scenario, the study examined two photo-molecularly imprinted adsorbents, M7 and M9. The competitive breakthrough curves of (E)-resveratrol and (E)-ε-viniferin were modelled, with all adsorption processes conducted at a controlled temperature of 15 °C. Furthermore, the fitting of the models was evaluated by calculating the correlation coefficient (R^2), the root-

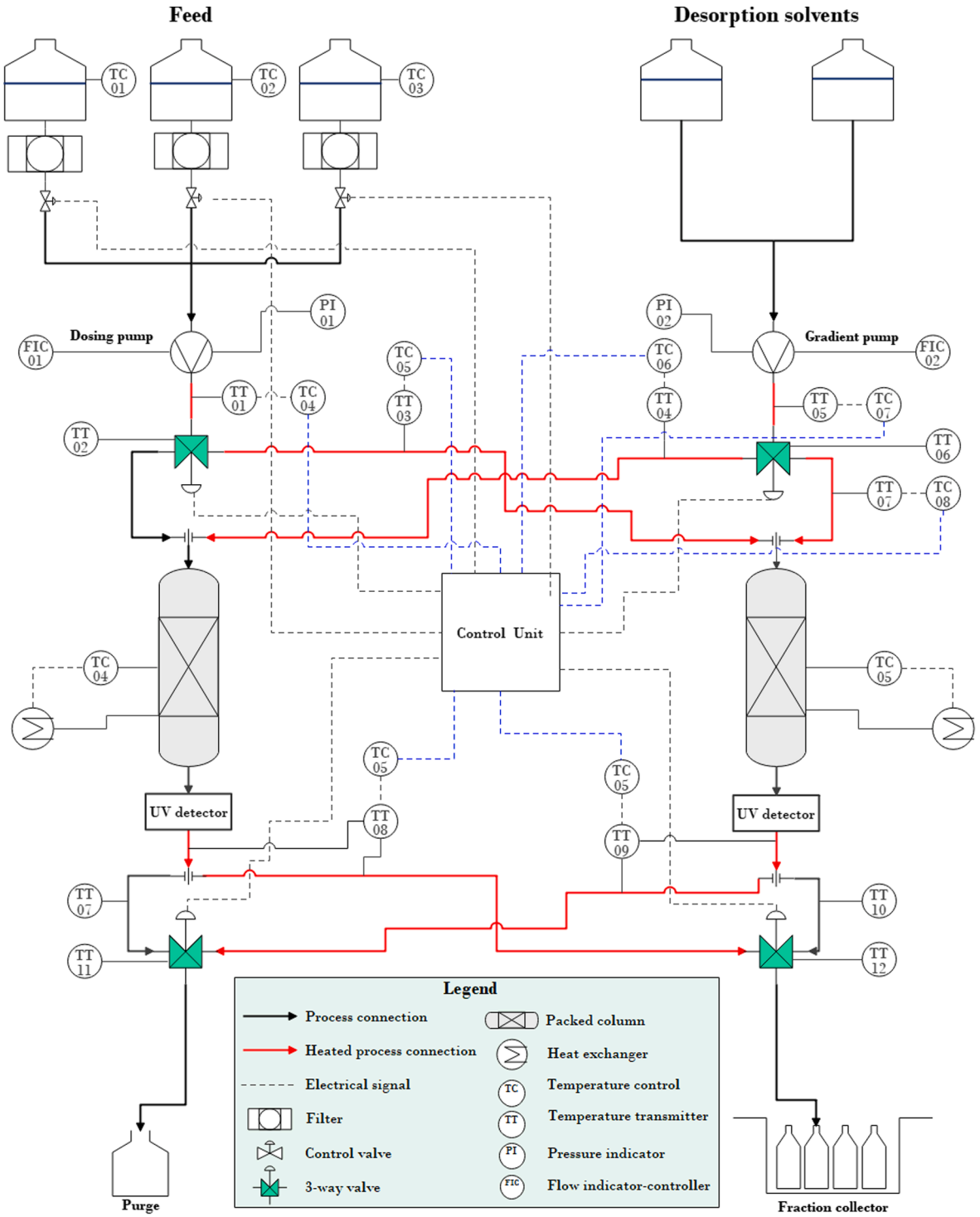

Fig. 2. Piping and instrumentation diagram of the adsorption–desorption prototype.

mean square root (RMSE) and the Akaike information criteria (AIC).

2.7. Purification procedure

An extract of grape stems in ethanol/water (80:20, v/v) was fed to the column, set to 15 °C, containing the synthesized MIP (either M7 or M9). The total volume of the extract was 500 mL, and the feeding was conducted in a recycled manner (the column's outlet goes directly to the extract's recipient) for approximately 92 bed volumes (one bed volume is 15.7 mL). Notice that prior to feeding the extract, the MIP was first equilibrated with ethanol/water (80:20, v/v). The pressure and temperature profiles of both M7 and M9 columns were recorded during this adsorption phase to ensure no system failures had occurred.

Throughout the entire desorption process, the MIP-packed column was consistently heated to 45 °C and kept at this temperature. The desorption sequence commenced with acidic water (pH = 3, 100 mL) followed by neutral water (100 mL). Subsequently, a series of water–ethanol mixtures was employed to efficiently desorb the retained compounds, employing the following proportions: 60–40 % (240 mL), 40–60 % (240 mL), and 20–80 % (240 mL). Finally, a desorption was

Table 3
Analytical kinetic models used in this study.

Kinetic model	Model equation
Logistic[1]	$\frac{C}{C_0} = \frac{1}{1+\exp(a-bt)}$
Wolborska[2]	$\frac{C}{C_0} = \exp(At - B)$
Clark	$\frac{C}{C_0} = (\frac{1}{1+B^*\exp(-rt)})^{\frac{1}{n-1}}$
Gompertz	$\frac{C}{C_0} = \exp[-\exp(\alpha_G - \beta_G t)]$
Log-Gompertz	$\frac{C}{C_0} = \exp[-\exp(\alpha_G - \beta_G \ln t)]$

[1] The unified logistic model encompasses Bohart-Adams, Thomas and Yoon-Nelson models. [2]Where $A = \frac{\varepsilon_b \beta C_0}{\rho q_F}$ and $B = \frac{\beta Z}{v}$.

Table 4
Parameters of the logistic functions.

Kinetic model	a	b
Bohart-Adams model	$\frac{K_{BA}N_0 Z}{v}$	$K_{BA}C_0$
Thomas model	$\frac{K_{Th}q_F m}{Q}$	$K_{Th}C_0$
Yoon-Nelson model	$K_{YN}\tau$	K_{YN}

made with ethanol (240 mL) followed by a washing phase of the material using methanol-acetic acid (9:1, v/v). The rationale for the desorbing solvents is further explained in the results and discussion part.

The desorbed fractions were primarily analysed by HPLC to estimate the eluted stilbenes. Thus, the recovery of each stilbene compound was determined relatively to their total adsorbed amount on the adsorbent (M7 or M9). Equation (1) was used to calculate the recovery. The term $m^i_{Fraction}$ is the mass of the compound "*i*" in the desorbed fraction and $m^i_{Adsorbed}$ corresponds to its mass in the adsorbed material.

$$R(\%) = 100\frac{m^i_{Fraction}}{m^i_{Adsorbed}} \quad (1)$$

Afterwards, the fractions were lyophilized and redissolved in their respective solvents. This allowed to ascertain the purity of two main stilbenes encountered in grape stems, namely (E)-resveratrol and (E)-ε-viniferin, as determined by the following equation:

$$P(\%) = 100\frac{C_i}{C_{sd}} \quad (2)$$

C_i (mg/L) is the concentration of (E)-resveratrol or (E)-ε-viniferin in the lyophilized-desorbed fraction and C_{sd} (mg/L) is the concentration of the residual solid resulting from the lyophilization of the fraction. Moreover, the enrichment values for (E)-resveratrol or (E)-ε-viniferin in their native fractions was determined by equation (3):

$$E = \frac{P^i_{Fraction}}{P^i_{Extract}} \quad (3)$$

Where $P^i_{Fraction}$ is the purity of the compound "*i*" in the desorbed fraction and $P^i_{Extract}$ is its purity in the initial extract.

3. Results and discussion

3.1. Grape stems analysis

The presence of stilbenes in grape stems has been well-documented by various research groups, such as Vergara et al. [22] and by our research group [20], among others. This discovery holds substantial importance, considering that grape stems are often discarded without specific utility. In this study, our research group has set a primary objective to purify selected stilbenes independently of the grape stems' origin. To this end, grapes stem samples sourced from the northern region of Portugal, a region renowned for its extensive grape plantations and wine production [23], were studied. Importantly, this research aims to provide insight into the variation of the content of stilbenes grape stem varieties using (E)-resveratrol as a proxy for this investigation. The extractions carried out in this study were solely based on hydroalcoholic solvents in opposition to our previous work where the extractions were carried out using acetonitrile [20].

For each extract, the concentration of (E)-resveratrol in the extract as well as the quantity per dry weight of grape stems were obtained and plotted in Fig. 3, and the corresponding chromatograms are shown in Fig. 4. At a first glance, it is evident that the origin and variety of the grape stems result in variations in (E)-resveratrol content within the plant matrix. Furthermore, the quantity of resveratrol per dry weight in the grapes stems of M–1 (harvest of 2021) was around 110 mg/kg dry weight, whereas in the grapes stems of the same region but from the harvest of 2023 (M–2) was around 11 mg/kg dry weight. This tenfold discrepancy between the two harvests can be attributed to factors such as climate, fertilizers and pesticides used in each harvest. However, this discrepancy can be also attributed to a phenomenon known to occur in post-pruning vine shoots, which is the accumulation of stilbenes in the grape stem's matrix along its storage time. These findings align with previous studies where the concentrations of (E)-resveratrol and (E)-ε-viniferin were shown to increase after months of storage [24,25]. To provide further insight into the diversity of phenolic profiles in these extracts, 3D chromatograms are presented in Figure S2.

It is essential to acknowledge that stilbenes' content in stored grape stems undergoes dynamic changes over time. This dynamic fluctuation is influenced by factors such as exposure to light, temperature, mechanical stress, and relative humidity, which may contribute to the de novo biosynthesis or to the degradation of stilbenes as outlined in previous works [26]. This phenomenon is further detailed in the study conducted by Craciun et al. where they had tracked the variation of (E)-resveratrol in vine shoots over a 90-day period. The study demonstrated a peak of (E)-resveratrol concentration after 75 days of vine shoots storage (1753.50 mg/kg dw); corresponding to a 20-fold increase compared to one week of storage (86.58 mg/kg dw) [27].

In fact, maintaining dark and cool conditions promotes a biochemical reaction wherein (E)-resveratrol transforms into (E)-ε-viniferin. This adds to the variability of the process in hand, as the extract employed in the designed process will consistently exhibit variations even when sourced from the same harvest year.

The geographical origin of the grapes significantly impacts the stilbenes' content in the stems. In fact, the samples collected from the northeast region, namely Douro (D) and Trás-os-Montes regions (T), contain more (E)-resveratrol than those from the region of Minho (M). This is imparted to the climate of the northeast region that puts more stress on the grape vines thus inducing the synthesis of more antioxidants to counter the adversities [28]. Studies have shown that grape varieties grown in regions with long winters and the possibility of snowfall exhibit higher content of phenolic compounds [29]. In general, various stress conditions induce an increase in stilbene levels in the vine both before and after pruning, particularly of the (E)-resveratrol compound [24,25,26,30].

Since the D-1 grape stems showed the highest content of (E)-resveratrol per dry weight, further extractions were carried out. After four extractions, the accumulated content of (E)-resveratrol surpassed 600 mg kg^{-1} dry weight as showcased in Fig. 5. From this latter, it can be observed that in the first extraction, the obtained amount of (E)-resveratrol was around 300 mg kg^{-1} dry weight. Along the subsequent three extractions, the amount was only doubled, which indicates diminishing returns when pursuing further extractions. While optimization of the extraction process lays beyond the scope of this study, this outcome indicates that successive extractions may not be economically

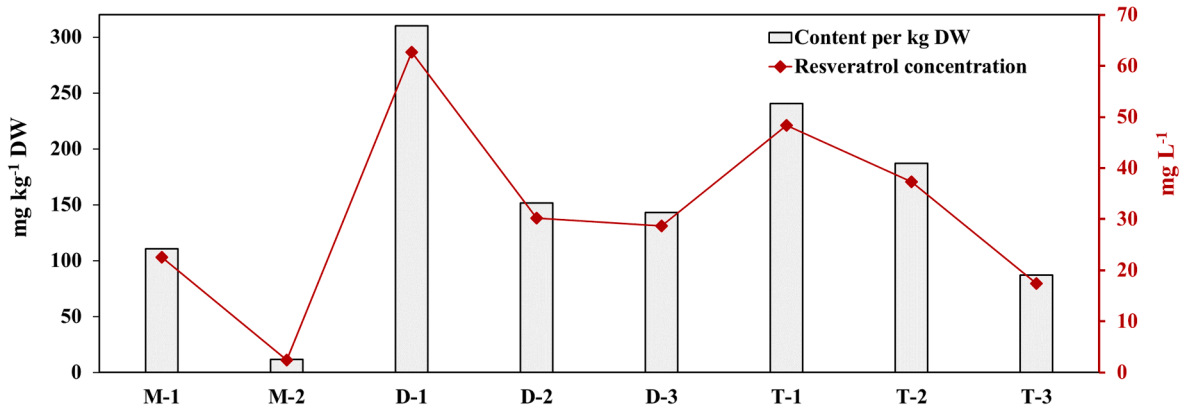

Fig. 3. Content of (E)-resveratrol in the different samples of grape stems. Both the content per dry weight and the extract concentrations are presented. The data refer to a single extraction.

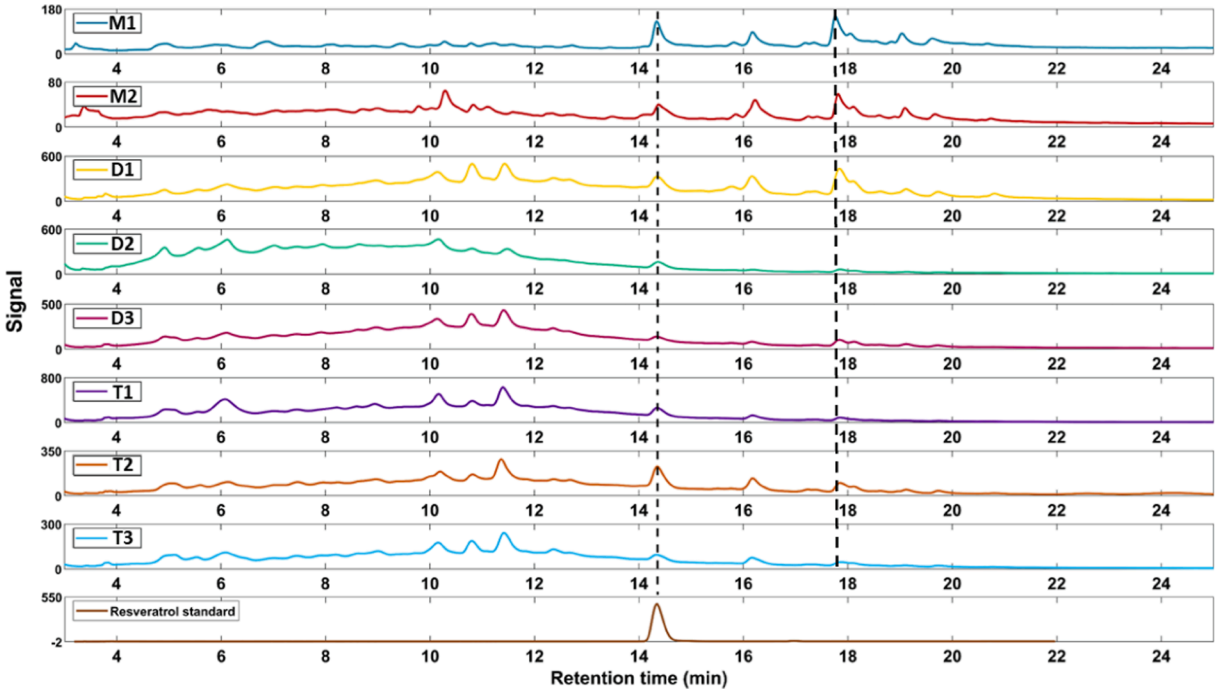

Fig. 4. HPLC-DAD chromatograms (280 nm) of grape stems extracts in comparison to the (E)-resveratrol standard. The (E)-ε-viniferin elutes around 18 min.

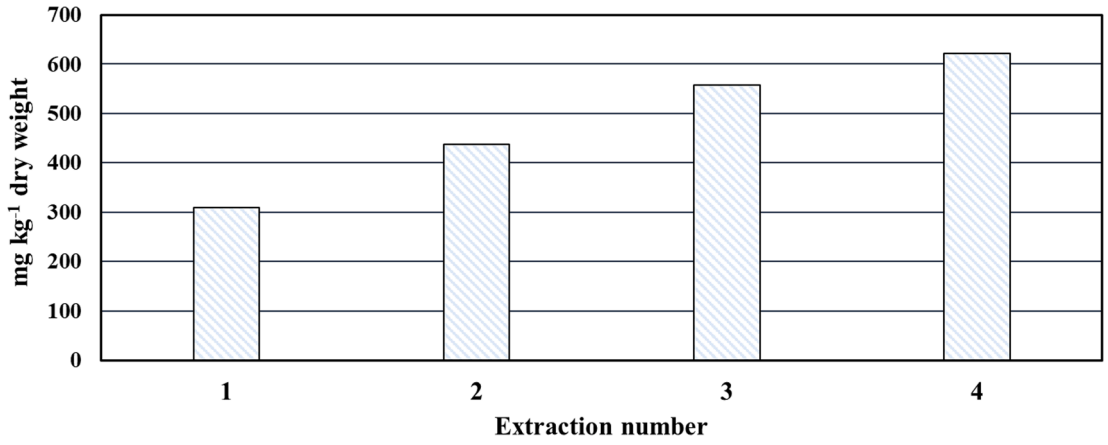

Fig. 5. Cumulative variation of the (E)-resveratrol content in the D-1 grape stems' sample after each extraction.

viable due to the potential hindrance of scaling up the purification process caused by the increased use of solvents.

To provide a comprehensive overview of stilbene content in vine biomass, relevant data from the literature was extracted and compiled in Table 5. This latter highlights the significant influence of the matrix, extraction technique, and solvent on the recovery of stilbenes. Additionally, other factors, such as the variety of the grapevine, year of harvest and growing conditions could alter these values. These variables explain why there are discrepancies in stilbene content across different studies in the literature.

Note that the exploitation of stilbenes from *Vitis vinifera* waste as a sustainable approach for the control of *Plasmopara viticola*, the agent causing grapevine downy mildew, was recently reported using enriched extracts from cane, wood, or root [9]. Enriched extracts with compositions varying between 1.3 % to 12.6 % in (E)-ε-viniferin and 1.1 % to 6.4 % in (E)-resveratrol were produced and tested for antifungal activity on *Plasmopara viticola*. The IC_{50} (concentration of the extract inhibiting 50 % of the disease development) were determined and values up to 60, 120 and 210 mg/L were observed with wood, root, and cane extracts, respectively. It's noteworthy that these values are comparatively higher than those obtained for purer stilbenes, such as 12, 70 and 110 mg/mL for r-viniferin, (E)-ε-viniferin and (E)-resveratrol, respectively. The elevated values for the extracts indicate the need for a more rigorous purification process for stilbenes, highlighting the trade-off between efficacy and the demanding purification required.

Notice that although the concentration of stilbenes in the root extract was the lowest, it demonstrated a highly potent antifungal bioactivity against *Plasmopara viticola*. This outcome may be attributed to the synergistic effect that can occur between stilbenes leading to an enhanced bioactivity [9].

Table 5
Stilbenes content in various vine biomass considering diverse extraction techniques.

Vine biomass	Extraction solvent and technique	(E)-Resveratrol (mg/kg dw biomass)	(E)-ε-Viniferin (mg/kg dw biomass)	Reference
Grape stems	Hydroalcoholic – UAE[(1)]	110	115.34	This work (M1)
Grape stems	Hydroalcoholic – UAE	12	14.7	This work (M2)
Grape stems	Hydroalcoholic – UAE	621.4	510.4	This work (D-1)
Grape stems	Acetonitrile – UAE	3700	_	[20]
Grape stems	Hydroalcoholic – Maceration	4700	1500	[31]
Grape stems	Methanol – Maceration	3200	1700	[32]
Grapevine canes	Hydroalcoholic – UAE	5590	868	[22]
Grapevine canes	Hydroalcoholic – Maceration	3450	1300	[33]
Grapevine canes	Acetone and water – Maceration	1070	2810	[34]
Grapevine canes	Chloroform, ethanol and water – Blended liquid–liquid extraction	_	60	[35]
Grapevine buds			90	
Grapevine shoots	Hydroalcoholic – Infusion	13984.7	4078.0	[36]
Grapevine shoots	Hydroalcoholic – UAE	5249.4	600.1	[37]
Grapevine shoots	Ethanol and diethyl ether – Maceration	1658.22	_	[27]
Grapevine leaves		43.54		
Grapevine tendrils		169.92		
Grape pomace	Hydroalcoholic – Hot-pressurized liquid extraction	4.28	_	[38]

[1]UAE: ultrasound-assisted extraction.

3.2. Molecularly imprinted adsorbents

The synthesis of the photo-molecularly imprinted polymers followed the methods outlined in our previous work [13], with a particular focus on scaling up the photo-polymerizations of M7 and M9. The polymerization process was carried out at room temperature under UV irradiation. The upscaled synthesis of the non-imprinted adsorbents was omitted in this study, given our prior findings demonstrating that the molecularly imprinted adsorbents exhibit superior binding capacities and selectivity towards (E)-resveratrol and its derivatives [13,20]. Photo-initiation permits to conduct the polymerization at room temperature, which is ideal for preserving the intermolecular interactions between the functional monomers of 4-vinylpyridine, styrene and (E)-resveratrol [14,15]. A scheme depicting this reaction is shown in Fig. 6.

Regarding the morphology of the MIP materials, SEM analysis was conducted and the corresponding images of both M7 and M9 are displayed in Fig. 7. These adsorbents exhibit a distinctive cluster of spherical particles. This morphology can be attributed to two primary factors. Firstly, the imprinting molecule of (E)-resveratrol compels polymerization to occur around it, leading to the formation of spherical particles, mainly drive by the thermodynamics of the multi-phase polymerization system. Secondly, the clustered appearance indicates the establishment of a polymeric network between these spherical parts, as expected after polymerization (precipitation polymerization in the dispersed phase). Additionally, the SEM image of M9 at 50 µm emphasizes the macroscopic three-dimensional nature of the photo-molecularly imprinted adsorbent.

3.3. Modelling of the dynamic adsorption

One of the study's objectives is to implement the technology of photo-molecularly imprinted adsorbents in the winemaking industry, using it as a tool to valorise the residues generated during wine production. To achieve this goal, an industrial prototype of a fixed-bed adsorption system was developed. This prototype serves as a suitable experimental framework for evaluating the effectiveness of the synthesized adsorbents in purifying valuable phenolic compounds from grape stems.

Two approaches are possible for carrying out the adsorption of stilbenes. The first approach involves feeding the grape stem extract through the inlet, while the outlet of the column is not processed again, hence the open-loop connotation. The second adsorption approach redirects the outlet of the adsorption column to the inlet, resulting in a recycled fixed-bed adsorption system. In both cases, the grape stems extract had an (E)-resveratrol concentration of 22.2 mg/L and 23.2 mg/L of (E)-ε-viniferin. For both scenarios, the data were fitted to kinetic analytical models, including the Logistic, Wolborska, Clark, Gompertz and Log-Gompertz models. Emphasis is placed on the recycling fixed-bed adsorption method, as this is the chosen approach for purifying stilbenes from grape stems.

3.3.1. Open-loop fixed-bed adsorption system

Fig. 8 showcases the global breakthrough obtained for both materials during an open-loop adsorption. The respective competitive breakthrough curves for (E)-resveratrol and (E)-ε-viniferin are also given in the same figure. At a first glance, the M9 appears to have a higher retention capacity since it reaches saturation after 21 bed volumes whereas the M7 only requires feeding the extract for 14 bed volumes.

The fitting of these competitive adsorption breakthrough curves is shown in Fig. 9. Based on the correlation coefficients (R^2) presented in Table 6, it is evident that the Logistic, Clark, Gompertz, and Log-Gompertz models consistently demonstrated high accuracy (R^2

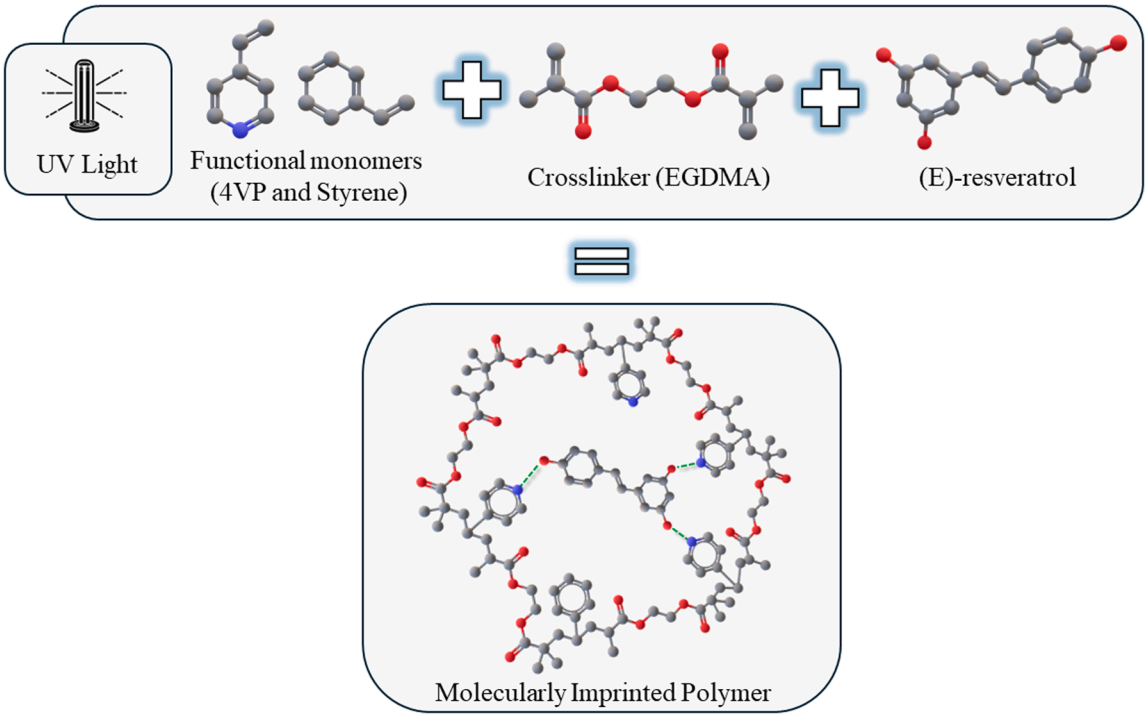

Fig. 6. Schematic representation of the MIP synthesis. This procedure was followed for both M7 and M9.

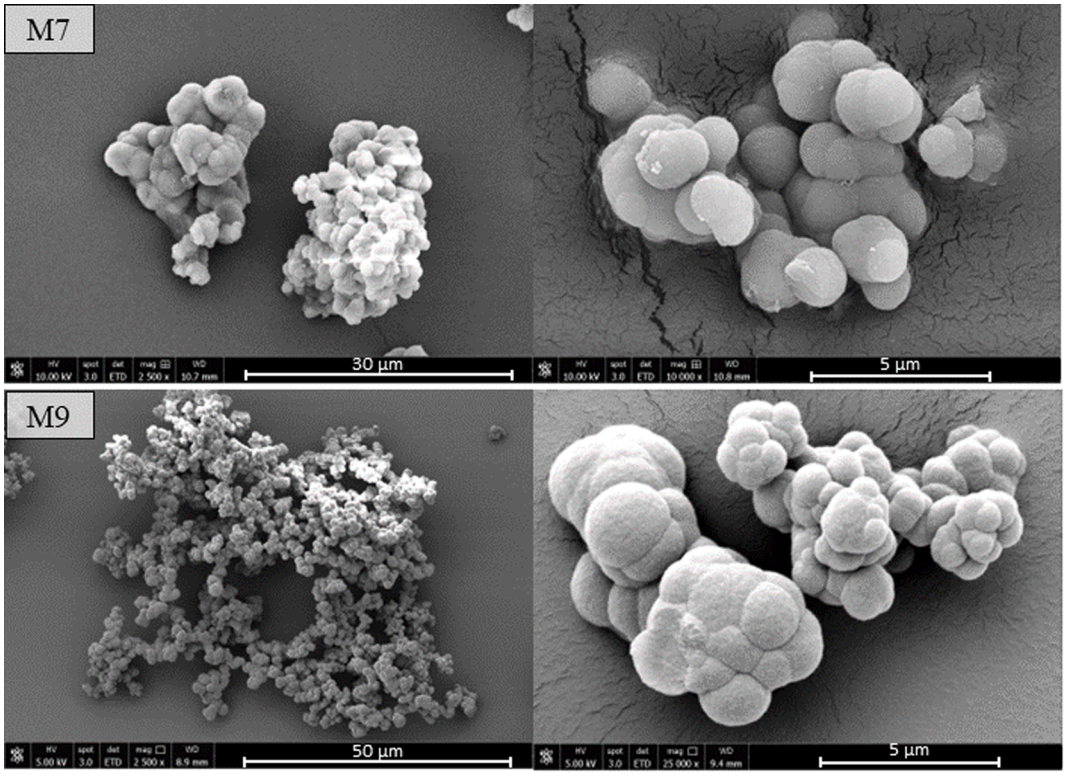

Fig. 7. SEM images showing the morphology of the MIP materials used in the purification of stilbenes from grape stem extracts. Upper images: M7, Lower images: M9.

ranging from 0.972 to 0.996) in predicting the experimental breakthrough curves for the open-loop fixed-bed adsorption of (E)-resveratrol and (E)-ε-viniferin on M7 and M9. Conversely, the Wolborska model consistently yielded lower correlation coefficients, suggesting potential limitations in accurately representing the adsorption behaviour. Specifically, regarding the M9 adsorbent, the Clark model exhibited a complete lack of agreement between its predictions and the observed concentrations. Despite rigorous attempts to refine initial conditions and optimize model parameters, pronounced discrepancies persisted. A thorough evaluation based on correlation coefficients, RMSE, and AIC

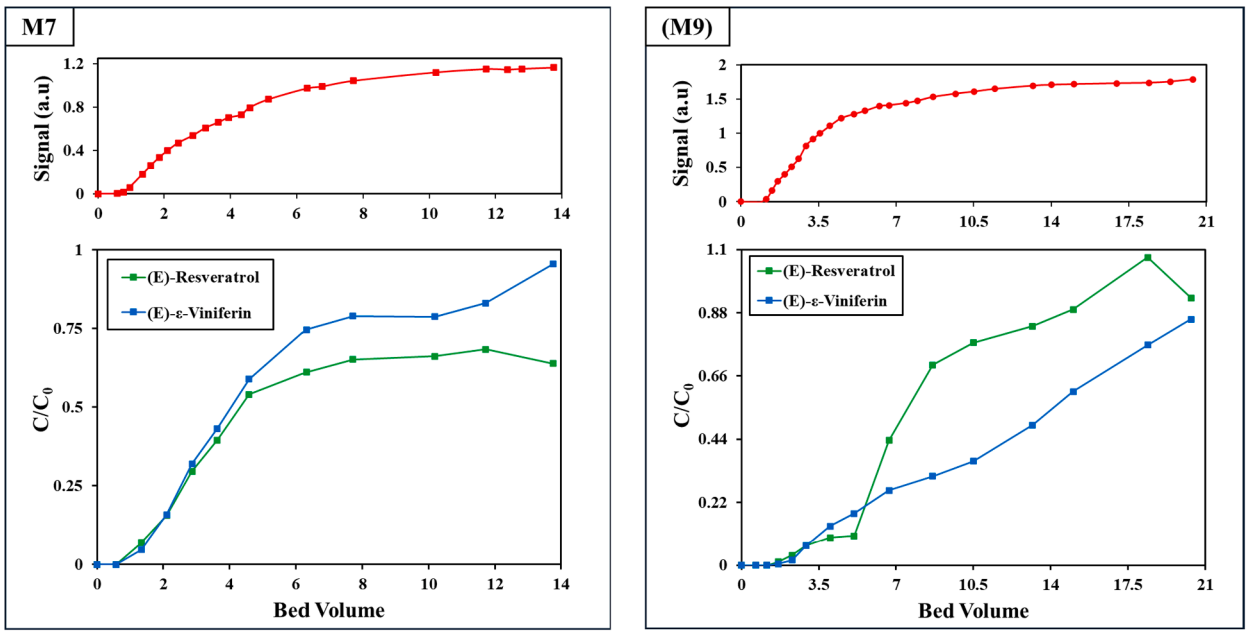

Fig. 8. Experimental breakthrough curves for the competitive adsorption of (E)-resveratrol and (E)-ε-viniferin in the M7 and M9 at 15 °C and a bed volume of 15.7 mL and a flowrate of 2 mL mn^{-1} in an open-loop fixed-bed adsorption system. The upper curves represent the global breakthrough obtained by monitoring the column's outlet at 450 nm.

values (refer to Table S1) indicates that the Gompertz model and its modified version, the Log-Gompertz model, emerge as the most suitable choices for fitting the experimental breakthrough curves. Further details regarding the fitted parameters are available in Table S2.

3.3.2. *Recycled fixed-bed adsorption system*

For the recycling fixed-bed adsorption experiments, the grape stem extract was passed through the column for a duration equivalent to 45 bed volumes. This value significantly surpasses the bed volumes utilized in the previous open-loop fixed-bed adsorption runs. The extended duration is intended to ensure that stilbenes reach an equilibrium concentration, effectively distributing between the adsorbent (M7 or M9) and the liquid phase. In this specific configuration, the outlet is recycled, eliminating any "waste" associated with the process. This approach ensures that the same initial volume of grape stems extract undergoes processing multiple times throughout the continuous operation. The fixed-bed adsorption prototype maintained the temperature of the MIP-packed columns at 15 °C during the recycling adsorption process. Fig. 10 illustrates the experimental breakthrough curves of the competitive adsorption of (E)-resveratrol and its dimer for both M7 and M9 adsorbents.

During the recycling adsorption process, the concentration of stilbenes in grape stems extract undergoes continuous variation. Thereby, reaching the inlet concentration (C_0) in the breakthrough curve of a specific compound becomes unattainable. Consequently, to address this challenge, the breakthrough curves of (E)-resveratrol and (E)-ε-viniferin are normalized using the equilibrium concentration (C_{eq}) instead of the inlet one. Furthermore, relying on the equilibrium concentrations as a normalization basis, facilitates the comparisons across different experiments. This approach reduces the dependency on the inlet concentration (C_0), which is inevitable when dealing with biomass extracts.

Moreover, treating crude biomass extracts introduces a challenge, as various compounds present in the extract can interfere with the adsorption process, resulting in a competitive retention on the MIP. This competition limits the available adsorption sites initially designed for the target compound. This phenomenon is expected to occur in molecularly imprinted polymers, as the imprinted sites can accommodate other molecules containing fragments of the imprinting molecule. In the case of M7 and M9, the molecular imprinting process utilized (E)-resveratrol as a template, leading also to the effective retention of (E)-ε-viniferin. This latter incorporates the (E)-resveratrol fragment into its structure as shown in Fig. 11. Understanding this outcome is crucial, as conventional fixed-bed adsorption studies rely on standards and known compounds that fail to capture the intricacies of biomass extracts [39,40].

The competitive breakthrough curves acquired in a recycled fixed-bed adsorption; were fitted to the analytical kinetic models as shown in Fig. 12. Their correlation coefficients are summarized in Table 7. For additional details on other calculated statistical parameters and fitted values, refer to Table S3 and S4 in the supporting information.

Based on the correlation coefficients provided in Table 7, along with the RMSE and AIC values provided in Table S3, it is clear that the Logistic, Clark, Gompertz, and Log-Gompertz models consistently demonstrated high correlation coefficients, ranging from 0.972 to 0.996, across all combinations of materials and compounds. These models exhibited a robust ability to predict the experimental breakthrough curves for the recycling fixed-bed adsorption process.

On the contrary, the Wolborska model consistently showed lower correlation coefficients compared to other models, indicating a weaker fit to the experimental data. This suggests that the Wolborska model may have limitations in accurately representing the adsorption behaviour of (E)-resveratrol and (E)-ε-viniferin on M7 and M9 in this experimental setup. The general non-fitting with the Wolborska model is due to the inherent nature of the model which is only suitable to represent the breakthrough curve at its initial stages ($C/C0 < 0.5$) [41]. Thus, this lack of fit suggests that the adsorption of (E)-resveratrol and (E)-ε-viniferin on the molecularly imprinted adsorbents is not controlled by film diffusion. This is logical considering the column drop that can nullify the effect of film diffusion and force the stilbenes to the bulk of the MIP, leading to a plug flow system [42,43].

Notably, the Log-Gompertz model stood out as particularly dominant, displaying near-perfect correlation coefficients of for the adsorption of (E)-resveratrol on M7 (0.992), the adsorption of (E)-resveratrol on M9 (0.996) and the adsorption of (E)-ε-viniferin on M9 (0.995). Furthermore, Log-Gompertz model had the lowest RMSE and AIC values (except for (E)-ε-viniferin adsorption on M7), thus emerging as a robust

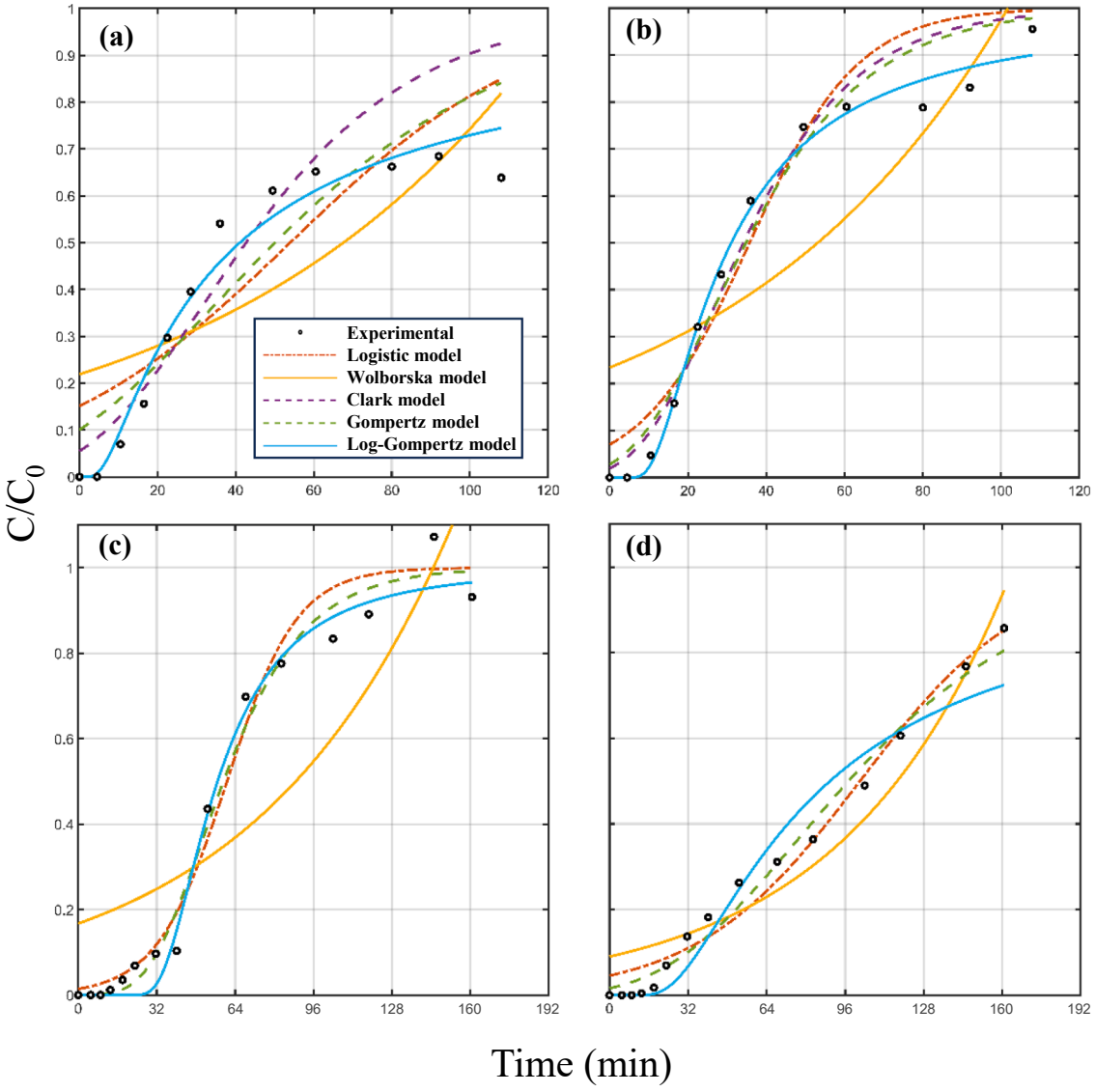

Fig. 9. Experimental and predicted breakthrough curves for M7 (a, b) and M9 (c, d) in an open-loop fixed-bed adsorption system. The breakthrough curves for (E)-resveratrol are depicted in the left figures (a and c), while those for (E)-ε-viniferin are illustrated in the right figures (b and d). Flowrate is equal to 2 mL min^{-1}.

Table 6
Correlation coefficients of the non-linear fitting of analytical models in case of an open-loop fixed-bed adsorption.

Kinetic model	M7_Res	M7_Vin	M9_Res	M9_Vin
Logistic	0.76	0.93	0.98	0.98
Wolborska	0.62	0.73	0.75	0.84
Clark	0.78	0.96	_	_
Gompertz	0.83	0.96	0.98	0.98
Log-Gompertz	0.97	0.99	0.99	0.96

choice for predicting breakthrough curves in this recycled fixed-bed adsorption configuration.

Among the analytical models examined in this research, the Log-Gompertz model demonstrated superior accuracy in reproducing the experimental data. The predicted breakthrough curves align with the experimental data throughout most of the experimental points, with a particular precision in the initial region of the curve where other models faltered. In fact, previous studies have also shown the superiority of the Log-Gompertz model in comparison to the Logistic and Clark models [44,41]. This is because the Log-Gompertz model is more appropriate to predict asymmetrical breakthrough curves as opposed to the other models which are more suitable to represent symmetrical sigmoidal breakthrough curves. Nevertheless, both Log-Gompertz and Gompertz models lack mechanistic insight, and their parameters do not offer valuable information about the adsorption process [41,45].

3.4. Purification of stilbenes

3.4.1. Rationale of the desorption

The desorption sequence initiated with mildly acidic water (pH = 3) facilitating the removal of a significant portion of hydrophilic compounds, including phenolic acids, oligosaccharides and to some extent some glycosylated polyphenols. Note that, the crude extracts of grape stems or grape canes also contain lignin, which related phenolic groups induce the retention of this heteropolymer in the 4VP adsorbents. Therefore, the pre-separation of lignin in the extracts using micro/nano-filtration (e.g.) will help with the increase of the purity of the target stilbene compounds obtained by sorption/desorption [46,47]. Compounds of low molecular weight with weaker binding capacity are easily eluted because are retained on the adsorbent in a non-specific manner, meaning that they are not trapped in the molecularly imprinted sites of

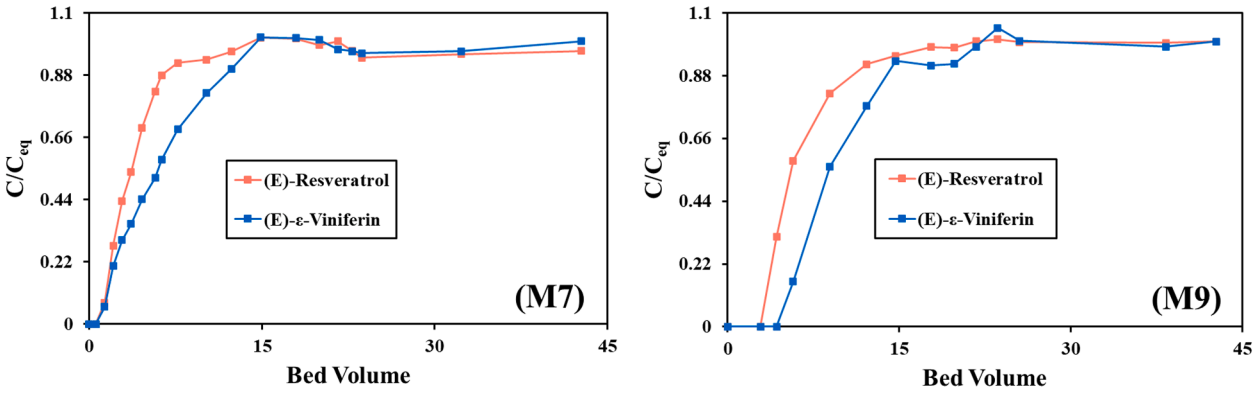

Fig. 10. Experimental breakthrough curves for the competitive adsorption of (E)-resveratrol and (E)-ε-viniferin in the M7 and M9 at 15 °C and a bed volume of 15.7 mL and a flowrate of 2 mL mn^{-1} in a recycled fixed-bed adsorption system.

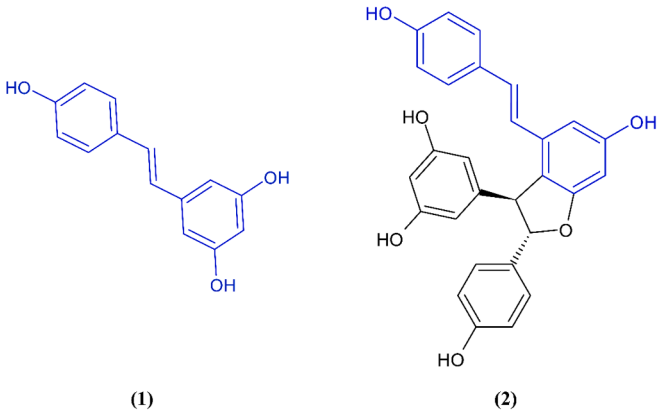

Fig. 11. Chemical structures of (E)-resveratrol (1) and its dimer (E)-ε-viniferin (2).

the adsorbent. Consequently, the neutral water is employed to ensure the elimination of any acetic acid traces in preparation for the subsequent desorption steps. Compositions of water and ethanol allow the elution of (E)-resveratrol or/and (E)-ε-viniferin, both of which have chemical structures depicted in Fig. 11. Due to its higher hydrophilicity compared to its derivative (E)-ε-viniferin, (E)-resveratrol is expected to elute with higher volumetric fractions of water. As the volumetric fraction of ethanol increases in the eluting solvent, more of (E)-viniferin elutes accompanied by a decrease of (E)-resveratrol elution. The chromatograms snippets of this phenomena are shown in Fig. 13 along with the diagram showing the steps of the desorption. Notice that although the photo-molecularly imprinted adsorbents were synthesized using (E)-resveratrol as a template, the retention of (E)-ε-viniferin was feasible due to the structural similarities shared between the two compounds.

3.4.2. *Stilbenes purification*

The purification of the stilbenes (E)-resveratrol and (E)-ε-viniferin was carried out by means of the fixed-bed adsorption prototype, as previously described. This purification process relied exclusively on water and ethanol mixtures during both the adsorption and the desorption phases. The decision to opt for cyclic adsorption is supported by the findings outlined in the modelling section. This choice is reinforced by our earlier research [20] which demonstrated the superior efficiency of recycled adsorption over the normal one.

In fact, recycled adsorption is a way to force (E)-resveratrol and its derivatives to get trapped in the photo-molecularly imprinted sites of the adsorbent. In a broader way, the recycled adsorption takes advantage of the dynamic combinatorial chemistry (DCC) [48], where various compounds undergo a systematic screening by the adsorbent until reaching a thermodynamic equilibrium. This equilibrium corresponds to the state wherein the target compounds, specifically (E)-resveratrol and (E)-ε-viniferin, are effectively retained by the adsorbent. This methodological approach emphasizes the effectiveness of recycled adsorption in selectively capturing and immobilizing the specified compounds, denoting a dynamic yet controlled molecular interaction.

During the adsorption phase, the column temperature was maintained at 15 °C. Conversely, when transitioning to the desorption phase, the column temperature was raised to 45 °C. This interplay of temperature between the two phases of the purification facilitates the retention and release of stilbenes into and from the matrix of the adsorbent. Since the material is based on 4-vinylpyridine, it interacts with the compounds through hydrogen bonding, a process sensitive to temperature. Therefore, this latter is set to 15 °C during the saturation phase to promote the retention of stilbenes. In contrast, it is increased to 45 °C during the elution phase to weaken the hydrogen bonding established between the adsorbent and the stilbenes. Further temperature increase is not recommended for two reasons: the potential degradation of stilbenes and the cost-efficiency of the process.

The recovery of the two stilbenes is illustrated in Fig. 14. Each stacked bar represents the compound's recovery and its distribution across the different desorbed fractions, namely 60 W (60 % water and 40 % ethanol), 40 W, 20 W and EtOH. Notably, the stacked bar chart excludes water fractions (acidic and neutral) since stilbenes do not elute in those. For both adsorbents M7 and M9, the highest recovery of (E)-resveratrol and (E)-ε-viniferin occurred in the 40 W and 20 W fractions. In the case of M7, the 60 W fraction exhibited modest recovery values, less than 5 % for both stilbene compounds, and even lower in the EtOH fraction (less than 1 %). Consequently, these two fractions do not warrant further investigation. Regarding the M9 adsorbent, the 60 W fractions had a recovery of 4.23 % for (E)-resveratrol and 0.86 % for (E)-ε-viniferin, indicating low recovery. Conversely, the ethanol (EtOH) fraction demonstrated a recovery exceeding the10% for (E)-ε-viniferin, inciting further analysis of this specific fraction, despite (E)-resveratrol's recovery being around 2 %.

Given the recovery values, specific fractions were carefully selected to assess the purity of the retrieved (E)-resveratrol and (E)-ε-viniferin. For the M7 adsorbent, the focus was on the 40 W and 20 W fractions, while for the M9 adsorbent, the analysis extended to the 40 W, 20 W, and EtOH fractions.

To accurately ascertain the gravimetric percentage of stilbenes in the acquired fractions, a crucial lyophilization step is essential. This process plays a key role in evaluating the purity of stilbenes in terms of weight percentage and by consequence their corresponding enrichments. In fact, directly calculating the enrichment of a compound without considering the impurities contained in the analysed sample could lead to misleading interpretations. An example of such inaccuracy is provided in the supporting information as Figure S3, where the enrichment

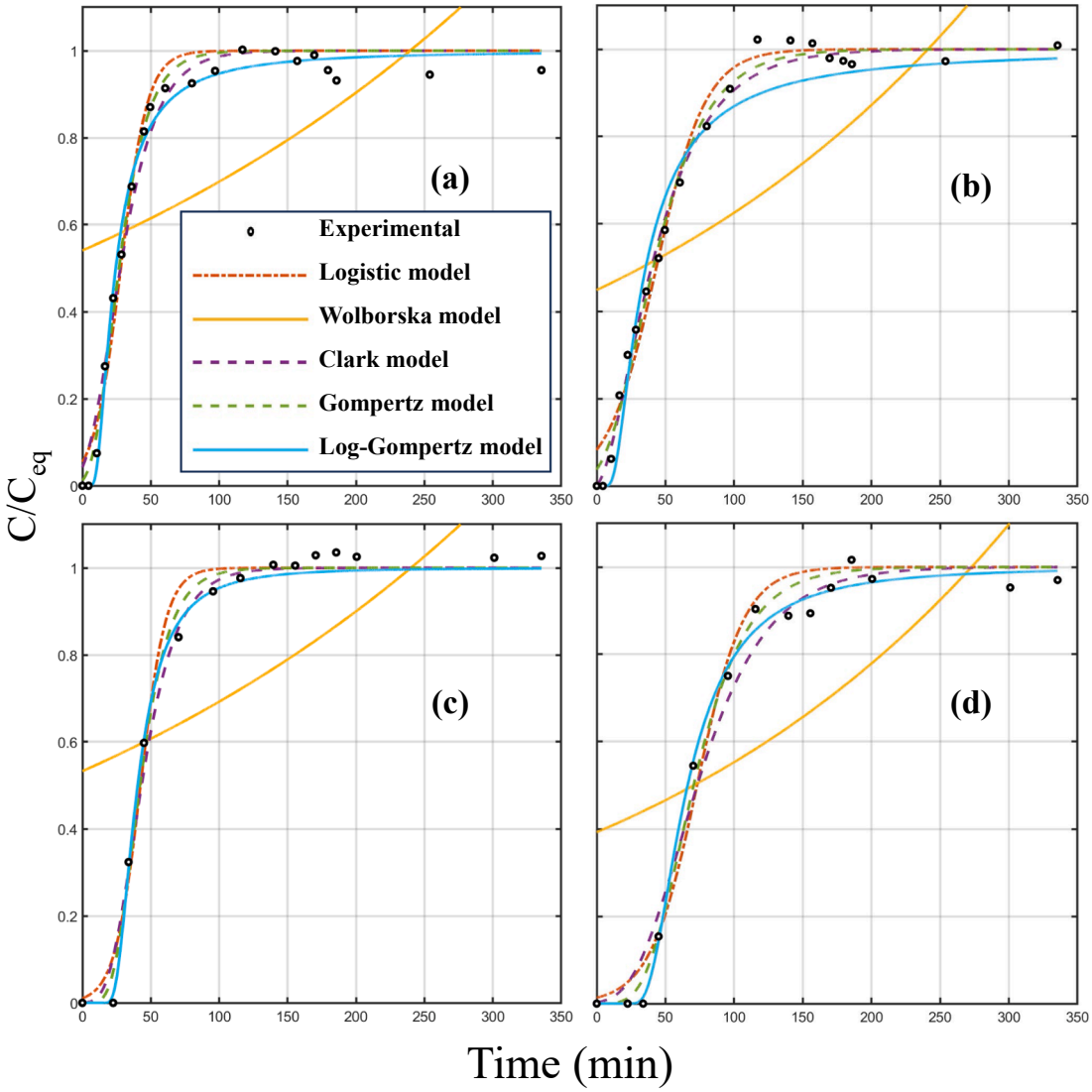

Fig. 12. Experimental and predicted breakthrough curves for M7 (a, b) and M9 (c, d) in a recycled fixed-bed adsorption system. The breakthrough curves for (E)-resveratrol are depicted in the left figures (a and c), while those for (E)-ε-viniferin are illustrated in the right figures (b and d). Flowrate is equal to 2 mL min^{-1}.

Table 7
Correlation coefficients values of the non-linear fitting of analytical models in case of a recycled fixed-bed adsorption.

Kinetic model	M7_Res	M7_Vin	M9_Res	M9_Vin
Logistic	0.981	0.984	0.983	0.980
Wolborska	0.358	0.496	0.426	0.485
Clark	0.983	0.993	0.989	0.982
Gompertz	0.990	0.991	0.991	0.990
Log-Gompertz	0.992	0.972	0.996	0.995

of both (E)-resveratrol and (E)-ε-viniferin are given in two distinct cases. The first case (Figure S3.a) accounts for the total mass of the sample (i.e. impurities included), and thus the resulting enrichment values are accurate. On the other hand (Figure S3.b) the enrichments of the two stilbenes are calculated by solely depending on the ratio of the peak areas of the compound to the total area of the chromatogram without considering other entities existing in the sample. The discrepancy of the enrichment values between the two approaches is as high as 10-fold, precisely demonstrating our thesis. Although the ratio of the areas can provide an indication about a compound's enrichment, it is not an accurate method, and gravimetric analysis should be conducted to obtain conclusive results.

The lyophilized fractions derived from the purification process, as depicted in Fig. 15, exhibit a discernible enhancement in purity when compared to the initial extract chromatogram. The primary constituents of these fractions are (E)-resveratrol and its dimer (E)-ε-viniferin, emphasizing the success of the purification process. However, as mentioned above, a mere comparison of chromatograms is insufficient to gain insight into the stilbenes' purification.

To address this limitation, the total mass of the lyophilized samples was considered, and the purities for both stilbenes, along with their corresponding enrichments, were determined and presented in Figs. 16 and 17. Notably, in all desorbed fractions, (E)-ε-viniferin exhibits a higher degree of purification than (E)-resveratrol, aligning with its initial higher purity in the extract.

The 20 % water fraction (20 W) and the ethanol fraction (EtOH) stand out as the optimal environments for (E)-ε-viniferin purification, achieving purities of 12.77 % and 9.77 % respectively. These values correspond to enrichments of 22.44 and 17.16, underlining the efficacy of these conditions. Conversely, the most favourable outcome for (E)-resveratrol purification is observed in the M9 fraction of 40 % water (40 W), attaining a purity of 3.4 %. This latter corresponds to an enrichment of nearly 9 folds.

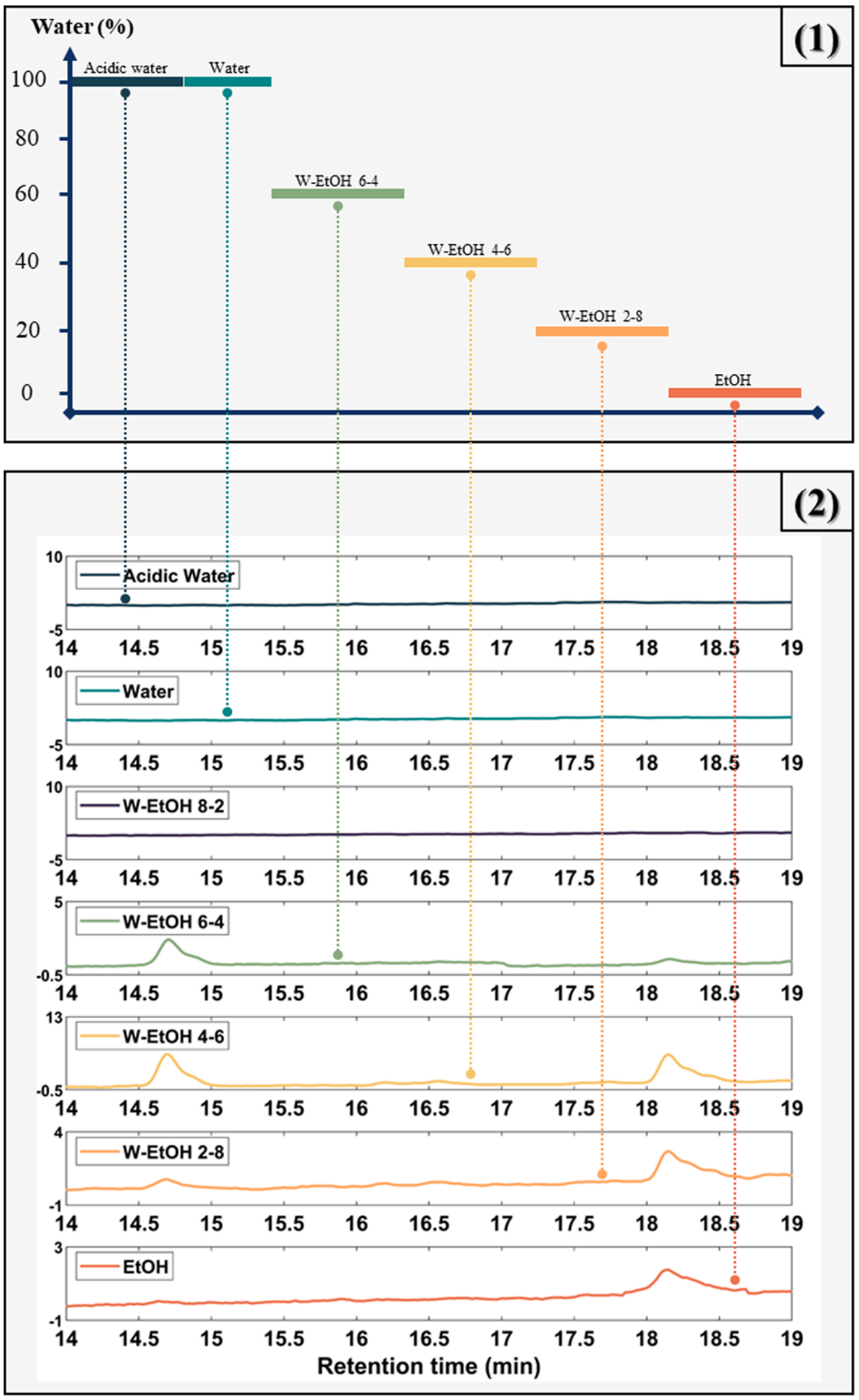

Fig. 13. (1) Elution sequence employed in the purification process; (2) Corresponding chromatograms highlighting the elution of (E)-resveratrol (t_R = 14.75 min) and (E)-ε-viniferin (t_R = 18.2 min) at 280 nm. The water–ethanol 8/2 (v/v) solvent composition does not elute neither (E)-resveratol nor (E)-ε-viniferin. Nevertheless, it is shown to validate the choice of the desorption solvents chosen.

These results highlight the superiority of M9 over M7, attributed to the higher crosslinker content in M7 (Y_{CL} = 60 %) compared to M9 (Y_{CL} = 40 %). Consequently, the polymer chains of M9 contain more 4VP units, enhancing the interaction of the adsorbent with the stilbenes.

In a previous publication, we achieved high purities of (E)-resveratrol nearing 90 % [20]. However, the extraction and adsorption processes in that study utilized acetonitrile from grape stems extract, a non-environmentally friendly chemical linked to adverse health effects upon exposure [49]. To address this concern, the current purification method exclusively employs ethanol–water mixtures for the extraction, adsorption, and desorption steps. Consequently, a decrease in selectivity towards (E)-resveratrol and a reduced binding capacity are anticipated.

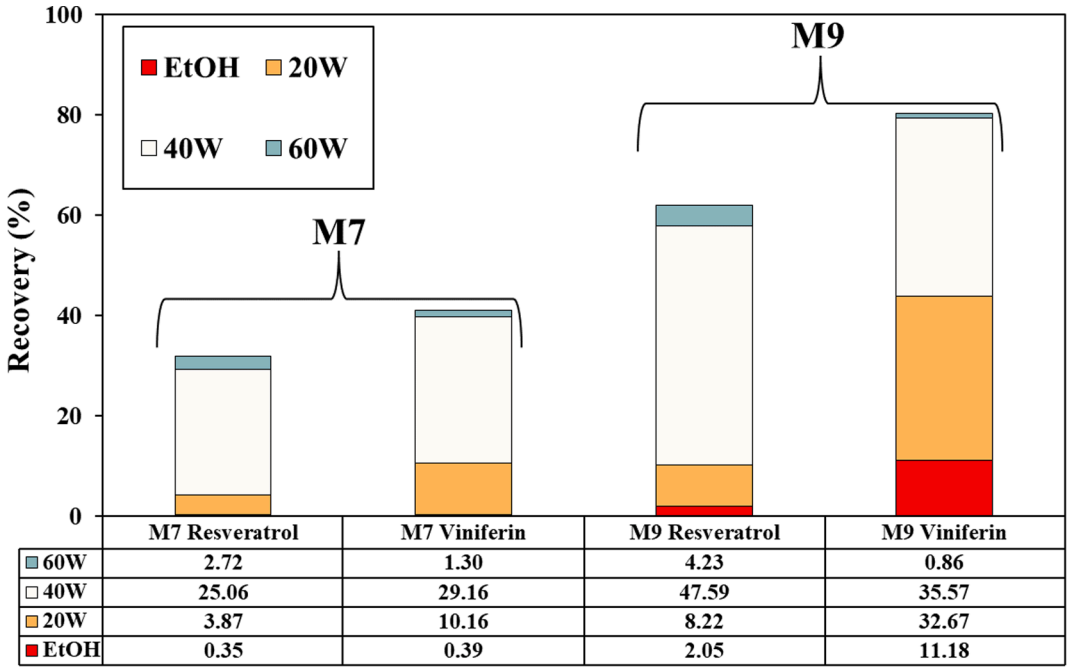

	M7 Resveratrol	M7 Viniferin	M9 Resveratrol	M9 Viniferin
60W	2.72	1.30	4.23	0.86
40W	25.06	29.16	47.59	35.57
20W	3.87	10.16	8.22	32.67
EtOH	0.35	0.39	2.05	11.18

Fig. 14. Recoveries of (E)-resveratrol and (E)-ε-viniferin in four distinct fractions, ranging from 60 % water (60 W) to 100 % ethanol (EtOH), employing the photo-molecularly imprinted adsorbents M7 and M9.

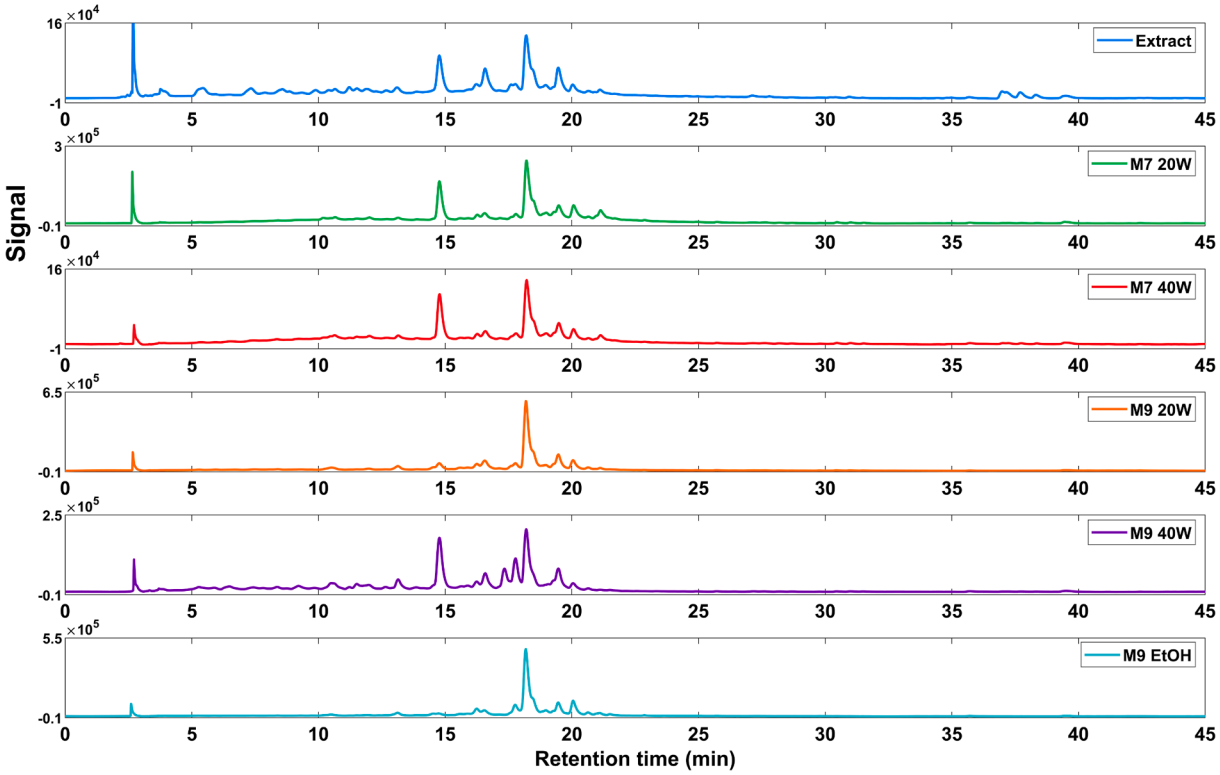

Fig. 15. HPLC-DAD of the lyophilized fractions resulting from the purification of grape stems extract using M7 and M9 (280 nm).

Given that the 4-vinylpyridine-based adsorbents rely on hydrogen bonds to retain (E)-resveratrol and its derivatives, the introduction of polar protic media like water and ethanol initiates interactions with the adsorbent, thereby diminishing available sites for stilbenes retention.

Table 8 presents a non-exhaustive list of different techniques utilized to purify one or more stilbenes from plant-based matrices. This table provides an overview of the current state-of-the-art in stilbenes' purification technology, emphasizing the types of solvents involved in the purification process. Furthermore, the reported purities in the table vary, with some techniques relying directly on HPLC chromatograms as an indicator of stilbene's purity without considering the weight percentage of the stilbene in the analyzed sample. Therefore, a distinction was made by introducing two purity terms: P_{HPLC}, denoting the ratio of the stilbene's area to the total chromatogram area, and P_{Sd}, representing

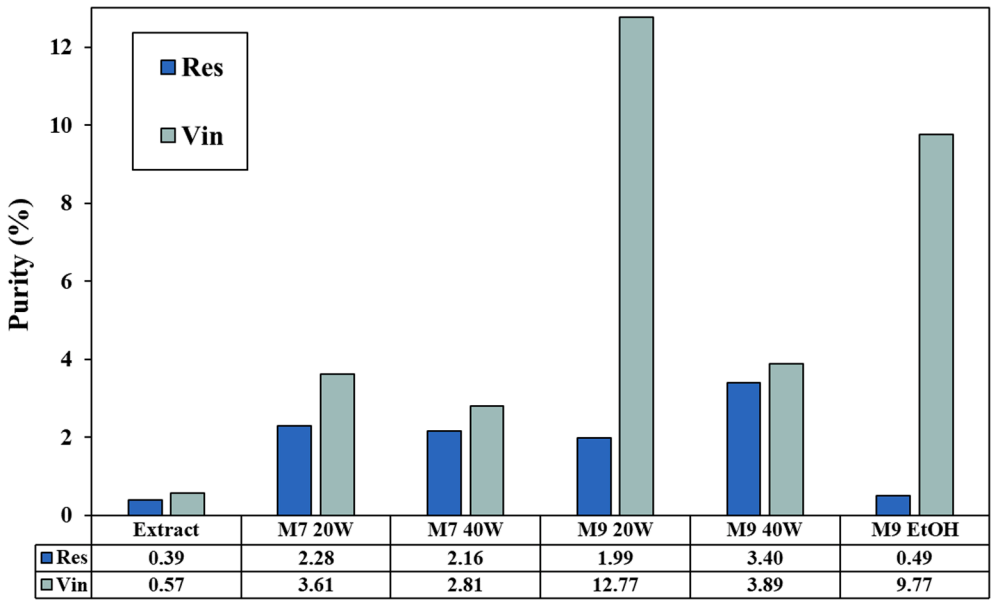

	Extract	M7 20W	M7 40W	M9 20W	M9 40W	M9 EtOH
Res	0.39	2.28	2.16	1.99	3.40	0.49
Vin	0.57	3.61	2.81	12.77	3.89	9.77

Fig. 16. Purities of (E)-resveratrol (Res) and (E)-ε-viniferin (Vin) in the eluted hydro alcoholic fractions compared to their initial purities in the grape stems extract.

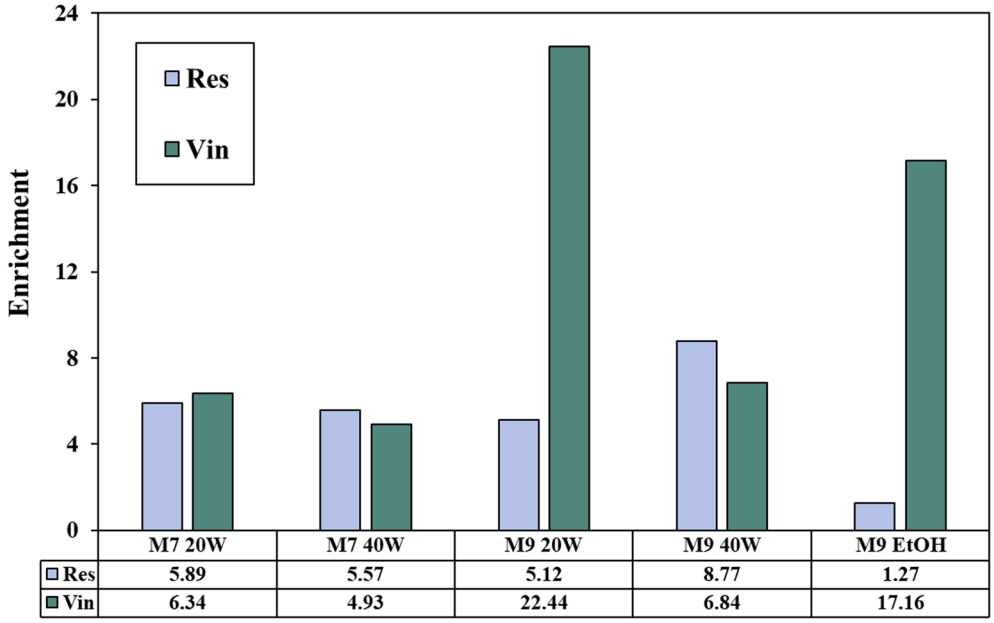

	M7 20W	M7 40W	M9 20W	M9 40W	M9 EtOH
Res	5.89	5.57	5.12	8.77	1.27
Vin	6.34	4.93	22.44	6.84	17.16

Fig. 17. Enrichments of (E)-resveratrol (Res) and (E)-ε-viniferin (Vin) in the eluted hydro alcoholic fractions.

the mass of the stilbene divided by the total mass of the sample. In comparing various stilbene purification techniques, the current study exhibits distinct features. Notably, the exclusive use of eco-friendly hydroalcoholic mixtures as solvents sets it apart from other methodologies that often rely on one or more potentially toxic solvents (e.g., chloroform, petroleum ether, methanol etc.). Besides, the purification process developed here relies on dynamic adsorption–desorption, prioritizing simplicity and minimizing the steps involved in stilbenes' isolation. In contrast, many other purification processes involve more complex techniques combined with the use of various commercial adsorbents. Additionally, the selection of grape stems, a byproduct of winemaking, as the matrix source reflects a sustainable approach by repurposing biomass residues. In fact, most of the studies presented in Table 8 (and in general), focus on the isolation of stilbenes from fresh plant matrices. While developing such processes is praiseworthy, it overlooks the sustainability aspect, as stilbenes can be found in different biomass residues.

It is important to highlight that the achieved purities within the enriched fractions of stilbenes, such as 12.8 % for (E)-ε-viniferin and 3.4 % for (E)-resveratrol, as previously mentioned, align with their potential application for controlling *Plasmopara viticola*. This relevance is particularly evident in light of the documented findings in this domain [9].

Hence, the photo-molecularly imprinted adsorbents synthesized in this study and in combination with the developed automated purification process are key to enrich stilbenes in a continuous manner independently of initial vine biomass composition and irrespective to its provenance. The results presented herein support the industrial implementation of an efficient purification process, especially that the proposed automated process does not include complicated operational units, making it easily adoptable on the industrial level. This endorses a more environmentally friendly approach that yields sustainable phytochemicals.

Table 8
Techniques used to isolate and purify stilbene compounds from different plant matrices.

Separation technique(s) and involved adsorbent(s)	Target stilbene(s)	Matrix type	Solvents used	Efficiency metric(s)	Reference
• Dynamic adsorption–desorption. • Photo-molecularly imprinted polymer.	(E)-ε-vinifierin	Grape stems	Hydroalcoholic mixtures	P_{Sd} = 12.77 % E = 22.44 R = 80.3 %	This work
	(E)-resveratrol			P_{Sd} = 3.4 % E = 8.77 R = 62.1 %	
• Dynamic adsorption–desorption. • Photo-molecularly imprinted polymer.	(E)-resveratrol	Grape stems	Acetonitrile for the adsorption and hydroalcoholic mixtures for the desorption	P_{Sd} = 87 % E = 3 R = 23.8 %	[20]
• Dynamic adsorption–desorption. • Macroporous resin – AB-8 (ethylstyrene based).	2,3,5,4′-Tetrahydroxystilbene-2-O-β-D-glycoside	Extract of *Polygonum multiflorum* roots	Hydroalcoholic mixtures	P_{Sd} = 64.76 % R = 68.34 % E = 8.6	[50]
• High-speed countercurrent chromatography and preparative HPLC. • YMC-Pack ODS-A (commercial adsorbent).	2,3,5,4′-Tetrahydroxystilbene-2-O-β-D-glycoside Piceatannol Resveratrol Isorhapontigenin Polydatin	Roots of *Polygonum multiflorum*	Petroleum ether, ethyl acetate, methanol and water	P_{HPLC} > 90 %	[51,52]
• Centrifugal Partition Chromatography • Repeated semipreparative HPLC runs (C-18 column).	(E)-resveratrol (E)-ε-vinifierin (E)-piceatannol Vitisin B Ampelopsin A Homodimers (pallidol, (E)-δ-viniferin, and (E)-ω-viniferin) Scirpusin A	*Vitis vinifera* L. Pinot Noir grape canes	Heptane, ethyl acetate, methanol, water and acetonitrile.	P_{HPLC} > 90 %	[3]
• Negative-pressure cavitation coupled with aqueous two-phase extraction.	longistyline C	Pigeon pea leaves	Ammonium sulfate, ethanol, and methanol	P_{Sd} = 2.2 % E = 2.27;	[52]
	Cajaninstilbene acid			P_{Sd} = 4.55 % E = 1.94	
• Two-step centrifugal partition chromatography.	Pinosylvin	Maritime pine knots	Petroleum ether, ethyl acetate, hydroalcoholic mixture, n-heptane, ethyl acetate, methanol, and water	P_{HPLC} = 91.4 %	[53]
	Pinosylvin methyl ether			P_{HPLC} = 91.1 %	
• Counter-current chromatography.	*trans*-δ-Viniferin	Grape stems	Methanol, ethyl acetate, n-hexane, methanol, and water	P_{HPLC} = 97.5 %	[54]
	trans-ε-Viniferin			P_{HPLC} = 93.2 %	
• Medium pressure liquid chromatography; semipreparative HPLC; recycling HPLC. • Series of commercial columns: Hi-flash MPLC; Gemini-NX C18; Synergi® Hydro-RP; Genesis™ C18; JAIGEL-ODS-AP	Oligostilebens (ex. ε-viniferin, *cis*-ε-viniferin, and *cis*-miyabenol C etc.)	Dipterocarpaceae	n-Hexane, acetone, ethyl acetate, methanol, water, and acetonitrile	P_{HPLC} > 90 %	[55]
• Preparative chromatography; high-speed counter-current chromatography. • Macroporous resin D101.	*trans*-Rhapontin,	*Rheum tanguticum Maxim. Ex Balf.*	Petroleum ether, ethanol, ethyl acetate, n-butanol, chloroform, methanol, and water	P_{HPLC} = 99.6 %	[56]
	cis-Rhapontin			P_{HPLC} = 97.2 %	
	trans-Desoxyrhaponticin			P_{HPLC} = 99.2 %	
• Preparative chromatography; high-speed counter-current chromatography. • Macroporous resin AB-8 MR.	(E)-Resveratrol-3-O-glucoside	Radix of *Polygonum cillinerve*	Ethanol, petroleum ether, ethyl acetate, n-butanol, chloroform, methanol, and water	P_{HPLC} = 99.1 %	[57]
	Pieceid-2 ''-O-gallate			P_{HPLC} = 97.8 %	
	(E)-Resveratrol			P_{HPLC} = 99.4 %	
• Ionic liquids-based microwave-assisted extraction.	3-Hydroxy-5-methoxystilbene-2-carbone acid Longistyline C Cajaninstilbene acid	Pigeon pea leaves	1-Alkyl-3-methylimidazolium ionic liquids	R = 95 %	[58]
• Preparative HPLC. • C18 column.	Vitisin A-13-O-β-D-glucoside	*Iris lactea*	Methanol, water and acetonitrile	P_{HPLC} = 90.1 % R = 0.685 %	[59]
	Vitisin D			P_{HPLC} = 95.5 % R = 0.105 %	
	Hopeaphenol			P_{HPLC} = 96.3 % R = 0.09 %	

(*continued on next page*)

Table 8 (*continued*)

Separation technique(s) and involved adsorbent(s)	Target stilbene(s)	Matrix type	Solvents used	Efficiency metric(s)	Reference
	Vitisin A			P_{HPLC} = 98.1 % R = 6.74 %	
• Dynamic adsorption–desorption. • Commercial resin HP-20.	(E)-Resveratrol	*Carménère* grape pomace	Hydroalcoholic mixtures	P_{Sd} = 0.13 % R = 8 %	[38]

P_{HPLC} represents the purity of the stilbene determined solely through chromatographic analysis (ratio of the stilbene's area to the total chromatogram area); P_{Sd} denotes the purity of the stilbene based on its weight percentage (ratio of the mass of the stilbene to the total sample mass); E is the enrichment factor of the stilbene and R represents the recovery of stilbene along the purification process.

4. Conclusions

The adsorption–desorption process developed in this study exclusively utilizes hydroalcoholic solvents, eliminating traceable toxic solvents. This method ensures the extraction of fractions enriched in (E)-resveratrol and (E)-ε-viniferin. The purification process was carried out in an automated manner through a fixed-bed adsorption prototype designed for precise control and monitoring. The purified fractions, containing both (E)-resveratrol and (E)-ε-viniferin, hold potential applications in various industries such as food, cosmetics, and as biological pesticides.

Although the final purities achieved for (E)-resveratrol and (E)-ε-viniferin are approximately 3.4 % and 12.8 %, respectively, these values might be considered low when analyzed in isolation. However, when considering their initial content in the crude extract of grape stems (0.39 % for (E)-resveratrol and 0.57 % for (E)-ε-viniferin), the enrichment is substantial, almost 23 times for (E)-ε-viniferin and 9 times for (E)-resveratrol. Furthermore, the developed adsorption–desorption process permits high recoveries of these two stilbenes considering that the crude extract of grape stems contains a myriad of other similar compounds. Recoveries exceeding 60 % and 80 % were obtained for (E)-resveratrol and (E)-ε-viniferin, respectively.

The kinetics of adsorption were investigated by fitting experimental data to analytical models, leading to the identification of the Log-Gompertz model as the best-fitting model for both recycled and open-loop fixed-bed adsorption. This preference is attributed to the nature of the Log-Gompertz equation, involving the logarithmic form of the time variable.

In summary, this study demonstrates the efficient purification of stilbenes by relying on hydroalcoholic solvents within the framework of a fixed-bed adsorption prototype. Meticulous consideration for compound affinity during desorption contributes to the success of the process. It is noteworthy that combining the developed process herein with other purification methods is feasible, potentially resulting in increased solvent usage and energy consumption.

The stilbene-enriched fractions obtained herein possess purities that fall within a suitable range to directly control the growth of *Plasmopara viticola* disease. Additionally, these enriched fractions can be combined to tailor novel environmentally friendly stilbene-containing phytochemicals with improved anti-fungal activity.

CRediT authorship contribution statement

Amir Bzainia: Writing – original draft, Validation, Investigation, Data curation. **Getúlio Igrejas:** Writing – review & editing, Supervision, Software, Conceptualization. **Maria João V. Pereira:** Writing – review & editing, Supervision, Software, Conceptualization. **Mário Rui P.F.N. Costa:** Writing – review & editing, Validation, Supervision, Conceptualization. **Rolando C.S. Dias:** Writing – review & editing, Validation, Supervision, Project administration, Funding acquisition, Conceptualization.

Declaration of competing interest

The authors declare that they have no known competing financial interests or personal relationships that could have appeared to influence the work reported in this paper.

Data availability

Data will be made available on request.

Acknowledgments

The authors are thankful for the financial aid provided by "BacchusTech-Integrated Approach for the Valorization of Winemaking Residues" (POCI-01-0247-FEDER-069583), supported by the Competitiveness and Internationalization Operational Program (COMPETE 2020), under the PORTUGAL 2020 Partnership Agreement, through the European Regional Development Fund (ERDF). A. Bzainia is grateful to the national funding by the Foundation for Science and Technology (FCT, Portugal) through the PhD grant of UI/BD/153688/2022. R.D. is grateful to the Foundation for Science and Technology (FCT, Portugal) for financial support through national funds FCT/MCTES (PIDDAC) to CIMO (UIDB/00690/2020 and UIDP/ 00690/2020) and SusTEC (LA/P/0007/2020). M.R.C. acknowledges the support by LA/P/0045/2020 (ALiCE), UIDB/50020/ 2020, and UIDP/50020/2020 (LSRE-LCM), funded by national funds through FCT/MCTES (PIDDAC). Getúlio Igrejas and Maria João Varanda Pereira work was supported by national funds through FCT/MCTES (PIDDAC): CeDRI, UIDB/05757/2020 (DOI: 10.54499/UIDB/05757/2020) and UIDP/05757/2020 (DOI: 10.54499/UIDP/05757/2020); and SusTEC, LA/P/0007/2020 (DOI: 10.54499/LA/P/0007/2020)

Appendix A. Supplementary data

Supplementary data to this article can be found online at https://doi.org/10.1016/j.seppur.2024.127798.

References

[1] S. Navarro-Orcajada, et al., Stilbenes: Characterization, bioactivity, encapsulation and structural modifications. A review of their current limitations and promising approaches, Crit. Rev. Food. Sci. Nutr. 63 (25) (Oct. 2023) 7269–7287, https://doi.org/10.1080/10408398.2022.2045558.

[2] B. De Filippis, A. Ammazzalorso, M. Fantacuzzi, L. Giampietro, C. Maccallini, R. Amoroso, Anticancer activity of stilbene-based derivatives, ChemMedChem 12 (8) (Apr. 2017) 558–570, https://doi.org/10.1002/cmdc.201700045.

[3] V. Sáez, et al., Oligostilbenoids in Vitis vinifera L. Pinot Noir grape cane extract: Isolation, characterization, in vitro antioxidant capacity and anti-proliferative effect on cancer cells, Food. Chem 265 (Nov. 2018) 101–110, https://doi.org/10.1016/j.foodchem.2018.05.050.

[4] H. Kim, K.-H. Seo, W. Yokoyama, Chemistry of pterostilbene and its metabolic effects, J. Agric. Food. Chem 68 (46) (Nov. 2020) 12836–12841, https://doi.org/10.1021/acs.jafc.0c00070.

[5] D. Bonnefont-Rousselot, Resveratrol and cardiovascular diseases, Nutrients 8 (5) (May 2016) 250, https://doi.org/10.3390/nu8050250.

[6] B. Tian, J. Liu, Resveratrol: a review of plant sources, synthesis, stability, modification and food application, J. Sci. Food. Agric 100 (4) (Mar. 2020) 1392–1404, https://doi.org/10.1002/jsfa.10152.

[7] M. Ferreira, M. Magalhães, R. Oliveira, J. Sousa-Lobo, I. Almeida, Trends in the use of botanicals in anti-aging cosmetics, Molecules 26 (12) (Jun. 2021) 3584, https://doi.org/10.3390/molecules26123584.

[8] T. Teka, L. Zhang, X. Ge, Y. Li, L. Han, X. Yan, Stilbenes: Source plants, chemistry, biosynthesis, pharmacology, application and problems related to their clinical Application-A comprehensive review, Phytochemistry 197 (May 2022) 113128, https://doi.org/10.1016/j.phytochem.2022.113128.

[9] J. Gabaston, et al., Stilbenes from *Vitis vinifera* L. Waste: A Sustainable Tool for Controlling *Plasmopara Viticola*, J. Agric. Food. Chem 65 (13) (Apr. 2017) 2711–2718, https://doi.org/10.1021/acs.jafc.7b00241.

[10] R. Pavela, P. Waffo-Teguo, B. Biais, T. Richard, and J.-M. Mérillon, "Vitis vinifera canes, a source of stilbenoids against Spodoptera littoralis larvae," *J Pest Sci (2004)*, vol. 90, no. 3, pp. 961–970, Jun. 2017, 10.1007/s10340-017-0836-1.

[11] J. Mosele, B.S. da Costa, S. Bobadilla, M.-J. Motilva, Phenolic composition of red and white wine byproducts from different grapevine cultivars from La Rioja (Spain) and how this is affected by the winemaking process, J. Agric. Food. Chem 71 (48) (Dec. 2023) 18746–18757, https://doi.org/10.1021/acs.jafc.3c04660.

[12] I. Pugajeva, I. Perkons, P. Górnaś, Identification and determination of stilbenes by Q-TOF in grape skins, seeds, juice and stems, J. Food Compos. Anal. 74 (Dec. 2018) 44–52, https://doi.org/10.1016/j.jfca.2018.09.007.

[13] A. Bzainia, R.C.S. Dias, M.R.P.F.N. Costa, Functionalization of polymer networks to target trans-resveratrol in winemaking residues supported by statistical design of experiments, Macromol. React. Eng 17 (4) (2023) Aug, https://doi.org/10.1002/mren.202200076.

[14] E.I. Paruli, O. Soppera, K. Haupt, C. Gonzato, Photopolymerization and photostructuring of molecularly imprinted polymers, ACS. Appl. Polym. Mater 3 (10) (Oct. 2021) 4769–4790, https://doi.org/10.1021/acsapm.1c00661.

[15] Q. Huang, et al., Flexible sponge ball-like temperature-responsive molecularly imprinted polymer with self-driven 'transformation recovery' and mechanism exploration, ACS. Appl. Polym. Mater 6 (2) (Jan. 2024) 1204–1214, https://doi.org/10.1021/acsapm.3c02132.

[16] A. Bzainia, R.C.S. Dias, M.R.P.F.N. Costa, Enrichment of quercetin from winemaking residual diatomaceous earth via a tailor-made imprinted adsorbent, Molecules 27 (19) (Sep. 2022) 6406, https://doi.org/10.3390/molecules27196406.

[17] R. Cao *et al.*, Surface molecularly imprinted polymers based on magnetic multi-walled carbon nanotubes for the highly selective purification of resveratrol from crude extracts of *Vitis vinifera* , *Arachis hypogaea* , and *Polygonum cuspidatum*, J. Sep. Sci., vol. 47, no. 4, Feb. 2024, 10.1002/jssc.202300811.

[18] C.P. Gomes, R.C.S. Dias, M.R.P.F.N. Costa, Fractionation of flavonols and anthocyanins in winemaking residues using molecularly imprinted cellulose-synthetic hybrid particles with pyridyl active surface, Nano Select (Feb. 2024), https://doi.org/10.1002/nano.202300153.

[19] A. Almeida, C. Martins, R.C.S. Dias, M.R.P.F.N. Costa, Competitive adsorption of phenolic acids, secoiridoids, and flavonoids in quercetin molecularly imprinted polymers and application for fractionation of olive leaf extracts, J. Chem. Eng. Data (Feb. 2024), https://doi.org/10.1021/acs.jced.3c00543.

[20] A. Bzainia, R.C.S. Dias, M.R.P.F.N. Costa, A simple process to purify (E)-resveratrol from grape stems with a photo-molecularly imprinted sorbent, Food. and. Bioproducts. Processing 142 (Nov. 2023) 1–16, https://doi.org/10.1016/j.fbp.2023.08.010.

[21] Q. Hu, S. Pang, D. Wang, Y. Yang, H. Liu, Deeper insights into the bohart-adams model in a fixed-bed column, J. Phys. Chem. B 125 (30) (Aug. 2021) 8494–8501, https://doi.org/10.1021/acs.jpcb.1c03378.

[22] C. Vergara, et al., stilbene levels in grape cane of different cultivars in southern chile: determination by HPLC-DAD-MS/MS method, J. Agric. Food. Chem 60 (4) (Feb. 2012) 929–933, https://doi.org/10.1021/jf204482c.

[23] Instituto da Vinha e do Vinho, https://www.ivv.gov.pt/np4/163.html, Evolução da Produção Nacional de Vinho por Região Vitivinícola Série 2009/2010 a 2022/2023.

[24] T. Gorena, V. Saez, C. Mardones, C. Vergara, P. Winterhalter, D. von Baer, Influence of post-pruning storage on stilbenoid levels in Vitis vinifera L. canes, Food. Chem 155 (Jul. 2014) 256–263, https://doi.org/10.1016/j.foodchem.2014.01.073.

[25] C. Cebrián, R. Sánchez-Gómez, M.R. Salinas, G.L. Alonso, A. Zalacain, Effect of post-pruning vine-shoots storage on the evolution of high-value compounds, Ind. Crops. Prod 109 (Dec. 2017) 730–736, https://doi.org/10.1016/j.indcrop.2017.09.037.

[26] S. Ferreyra, R. Bottini, A. Fontana, Temperature and light conditions affect stability of phenolic compounds of stored grape cane extracts, Food. Chem 405 (Mar. 2023) 134718, https://doi.org/10.1016/j.foodchem.2022.134718.

[27] A.L. Crăciun, G. Gutt, Study on kinetics of trans-resveratrol, total phenolic content, and antioxidant activity increase in vine waste during post-pruning storage, Appl. Sci. 12 (3) (Jan. 2022) 1450, https://doi.org/10.3390/app12031450.

[28] S. Kabtni, et al., Influence of climate variation on phenolic composition and antioxidant capacity of Medicago minima populations, Sci. Rep 10 (1) (May 2020) 8293, https://doi.org/10.1038/s41598-020-65160-4.

[29] R. Gutiérrez-Escobar, M.J. Aliaño-González, E. Cantos-Villar, Wine polyphenol content and its influence on wine quality and properties: a review, Molecules 26 (3) (Jan. 2021) 718, https://doi.org/10.3390/molecules26030718.

[30] K. Billet, et al., Mechanical stress rapidly induces E-resveratrol and E-piceatannol biosynthesis in grape canes stored as a freshly-pruned byproduct, Food. Chem 240 (Feb. 2018) 1022–1027, https://doi.org/10.1016/j.foodchem.2017.07.105.

[31] A. Aaviksaar, M. Haga, T. Püssa, M. Roasto, and G. Tsoupras, "Purification of resveratrol from vine stems, Proc. Estonian Acad. Sci. Chem., vol. 52, no. 4, p. 155, 2003, 10.3176/chem.2003.4.02.

[32] T. Püssa, J. Floren, P. Kuldkepp, A. Raal, Survey of grapevine *Vitis vinifera* stem polyphenols by liquid chromatography−diode array detection−tandem mass spectrometry, J. Agric. Food. Chem 54 (20) (Oct. 2006) 7488–7494, https://doi.org/10.1021/jf061155e.

[33] S. Rayne, E. Karacabey, G. Mazza, Grape cane waste as a source of trans-resveratrol and trans-viniferin: High-value phytochemicals with medicinal and anti-phytopathogenic applications, Ind. Crops. Prod 27 (3) (May 2008) 335–340, https://doi.org/10.1016/j.indcrop.2007.11.009.

[34] R.F. Guerrero, et al., Grapevine cane's waste is a source of bioactive stilbenes, Ind. Crops. Prod 94 (Dec. 2016) 884–892, https://doi.org/10.1016/j.indcrop.2016.09.055.

[35] S. Qsaib, N. Mateus, F.E. Ikbal, L.A. Rifai, V. de Freitas, T. Koussa, Direct identification and characterization of phenolic compounds from crude extracts of buds and internodes of grapevine (Vitis vinifera cv Merlot), Nat. Prod. Commun 9 (11) (2014), https://doi.org/10.1177/1934578X1400901110, pp. 1934578X1400901.

[36] I.V. Chernousova, G.P. Zaitsev, T.A. Zhilyakova, Y.V. Grishin, Biologically active agents as part of extracts of grape leaves and vine and method of their extraction, IOP. Conf. Ser. Earth. Environ. Sci 954 (1) (Jan. 2022) 012016, https://doi.org/10.1088/1755-1315/954/1/012016.

[37] M. Noviello, A.F. Caputi, G. Squeo, V.M. Paradiso, G. Gambacorta, F. Caponio, Vine Shoots as a Source of Trans-Resveratrol and ε-Viniferin: A Study of 23 Italian Varieties, Foods 11 (4) (Feb. 2022) 553, https://doi.org/10.3390/foods11040553.

[38] N.L. Huaman-Castilla, M. Martínez-Cifuentes, C. Camilo, F. Pedreschi, M. Mariotti-Celis, J.R. Pérez-Correa, The Impact of Temperature and Ethanol Concentration on the Global Recovery of Specific Polyphenols in an Integrated HPLE/RP Process on Carménère Pomace Extracts, Molecules 24 (17) (Aug. 2019) 3145, https://doi.org/10.3390/molecules24173145.

[39] D.M.R.E.A. Dissanayake, P.K.D. Chathuranga, P.I. Perera, M. Vithanage, M.C. M. Iqbal, Modeling of Pb(II) adsorption by a fixed-bed column, Bioremediat. J 20 (3) (Jul. 2016) 194–208, https://doi.org/10.1080/10889868.2016.1212808.

[40] J.B. Dima, M. Ferrari, N. Zaritzky, Mathematical Modeling of Fixed-Bed Columns Adsorption: Hexavalent Chromium onto Chitosan Flakes, Ind. Eng. Chem. Res 59 (34) (Aug. 2020) 15378–15386, https://doi.org/10.1021/acs.iecr.0c02004.

[41] D. Juela, M. Vera, C. Cruzat, X. Alvarez, E. Vanegas, Mathematical modeling and numerical simulation of sulfamethoxazole adsorption onto sugarcane bagasse in a fixed-bed column, Chemosphere 280 (Oct. 2021) 130687, https://doi.org/10.1016/j.chemosphere.2021.130687.

[42] F. Gritti, W. Piatkowski, G. Guiochon, Study of the mass transfer kinetics in a monolithic column, J. Chromatogr. A 983 (1–2) (Jan. 2003) 51–71, https://doi.org/10.1016/S0021-9673(02)01648-5.

[43] M.K. Al Mesfer, M. Danish, M.I. Khan, I.H. Ali, M. Hasan, A. El Jery, Continuous Fixed Bed CO2 Adsorption: Breakthrough, Column Efficiency, Mass Transfer Zone, Processes 8 (10) (Oct. 2020) 1233, https://doi.org/10.3390/pr8101233.

[44] K.H. Chu, Fitting the Gompertz equation to asymmetric breakthrough curves, J. Environ. Chem. Eng 8 (3) (Jun. 2020) 103713, https://doi.org/10.1016/j.jece.2020.103713.

[45] Q. Hu, D. Wang, S. Pang, L. Xu, Prediction of breakthrough curves for multicomponent adsorption in a fixed-bed column using logistic and Gompertz functions, Arab. J. Chem. 15 (9) (Sep. 2022) 104034, https://doi.org/10.1016/j.arabjc.2022.104034.

[46] R. Apolinar-Valiente, P. Williams, T. Doco, Recent advances in the knowledge of wine oligosaccharides, Food. Chem 342 (Apr. 2021) 128330, https://doi.org/10.1016/j.foodchem.2020.128330.

[47] D.P. Nogueira, et al., Evaluation of grape stems and grape stem extracts for sulfur dioxide replacement during grape wine production, Curr. Res. Food. Sci 6 (2023) 100453, https://doi.org/10.1016/j.crfs.2023.100453.

[48] J. Li, P. Nowak, S. Otto, Dynamic combinatorial libraries: from exploring molecular recognition to systems chemistry, J. Am. Chem. Soc 135 (25) (Jun. 2013) 9222–9239, https://doi.org/10.1021/ja402586c.

[49] G.S. Dotson, A. Maier, A. Parker, Immediately dangerous to life or health (IDLH) value profile : Acetonitrile (CAS® No. 75-05-8)," 2017.

[50] T. Deng, J. Jia, N. Luo, H. Li, A dual-task method for the simultaneous detoxification and enrichment of stilbene glycoside from Polygonum multiflorum roots extract by macroporous resin, Chem. Eng. J. 237 (Feb. 2014) 138–145, https://doi.org/10.1016/j.cej.2013.10.020.

[51] M. Liu, X. Li, Q. Liu, S. Xie, F. Zhu, X. Chen, Preparative isolation and purification of 12 main antioxidants from the roots of Polygonum multiflorum Thunb. using high-speed countercurrent chromatography and preparative HPLC guided by 1,1′-diphenyl-2-picrylhydrazyl-HPLC, J. Sep. Sci 43 (8) (Apr. 2020) 1415–1422, https://doi.org/10.1002/jssc.201901287.

[52] X.-Q. Wang, et al., Negative-pressure cavitation coupled with aqueous two-phase extraction and enrichment of flavonoids and stilbenes from the pigeon pea leaves and the evaluation of antioxidant activities, Sep. Purif. Technol 156 (Dec. 2015) 116–123, https://doi.org/10.1016/j.seppur.2015.09.028.

[53] J. Gabaston, et al., Separation and isolation of major polyphenols from maritime pine (Pinus pinaster) knots by two-step centrifugal partition chromatography monitored by LC-MS and NMR spectroscopy, J. Sep. Sci 43 (6) (Mar. 2020) 1080–1088, https://doi.org/10.1002/jssc.201901066.

[54] Q. Kong, X. Ren, R. Hu, X. Yin, G. Jiang, Y. Pan, Isolation and purification of two antioxidant isomers of resveratrol dimer from the wine grape by counter-current chromatography, J. Sep. Sci 39 (12) (Jun. 2016) 2374–2379, https://doi.org/10.1002/jssc.201600004.

[55] R. Ramli, N.H. Ismail, N. Manshoor, Recycling HPLC for the purification of oligostilbenes from Dipterocarpus semivestitus and Neobalanocarpus heimii (Dipterocarpaceae), J. Liq. Chromatogr. Relat. Technol 40 (18) (Nov. 2017) 943–949, https://doi.org/10.1080/10826076.2017.1386673.
[56] X. Zhao, F. Han, Y. Li, H. Yue, Preparative Isolation and Purification of Three Stilbene Glycosides from the Tibetan Medicinal Plant Rheum tanguticum Maxim. Ex Balf. by High-speed Counter-current Chromatography, Phytochem. Anal. 24 (2) (Feb. 2013) 171–175, https://doi.org/10.1002/pca.2397.
[57] X. Chi, Y. Xing, Y. Xiao, Q. Dong, F. Hu, Separation and purification of Three stilbenes from the radix of polygonum cillinerve (Nakai) Ohwl by macroporous resin column chromatography combined with high-speed counter-current chromatography, Quim. Nova (2014), https://doi.org/10.5935/0100-4042.20140256.
[58] Z. Wei, et al., Ionic liquids-based microwave-assisted extraction of active components from pigeon pea leaves for quantitative analysis, Sep. Purif. Technol 102 (Jan. 2013) 75–81, https://doi.org/10.1016/j.seppur.2012.09.031.
[59] F.-F. Tie, Y.-Y. Fu, N. Hu, Z. Chen, H.-L. Wang, Isolation of oligostilbenes from Iris lactea Pall. var. chinensis (Fisch.) Koidz and their anti-inflammatory activities, RSC Adv 12 (51) (2022) 32912–32922, https://doi.org/10.1039/D2RA05176A.